References

1. Norata GD and Catapano AL: Molecular mechanisms responsible for the anti-inflammatory and protective effect of HDL on the endothelium. Vasc Health Risk Manag 1: 119-129, 2005.
2. Nofer JR, Kehrel B, Fobker M, Levkau B, Assmann G and von Eckardstein A: HDL and arteriosclerosis: beyond reverse cholesterol transport. Atherosclerosis 161: 1-16, 2002.
3. Calabresi L, Gomaraschi M and Franceschini G: Endothelial protection by high-density lipoproteins: from bench to bedside. Arterioscler Thromb Vasc Biol 23: 1724-1731, 2003.
4. Norata GD, Callegari E, Inoue H and Catapano AL: HDL3 induces cyclooxygenase-2 expression and prostacyclin release in human endothelial cells via a p38 MAPK/CRE-dependent pathway: effects on COX-2/PGI-synthase coupling. Arterioscler Thromb Vasc Biol 24: 871-877, 2004.
5. Ferretti G, Bacchetti T, Negre-Salvayre A, Salvayre R, Dousset N and Curatola G: Structural modifications of HDL and functional consequences. Atherosclerosis 184: 1-7, 2006.
6. Norata GD, Pirillo A and Catapano AL: Modified HDL: biological and physiopathological consequences. Nutr Metab Cardiovasc Dis 2006.
7. Nakajima T, Origuchi N, Matsunaga T, Kawai S, Hokari S, Nakamura H, Inoue I, Katayama S, Nagata A and Komoda T: Localization of oxidized HDL in atheromatous plaques and oxidized HDL binding sites on human aortic endothelial cells. Ann Clin Biochem 37: 179-186, 2000.
8. Bergt C, Pennathur S, Fu X, Byun J, O'Brien K, McDonald TO, Singh P, Anantharamaiah GM, Chait A, Brunzell J, Geary RL, Oram JF and Heinecke JW: The myeloperoxidase product hypochlorous acid oxidizes HDL in the human artery wall and impairs ABCA1-dependent cholesterol transport. Proc Natl Acad Sci USA 101: 13032-13037, 2004.
9. Zheng L, Nukuna B, Brennan ML, Sun M, Goormastic M, Settle M, Schmitt D, Fu X, Thomson L, Fox PL, Ischiropoulos H, Smith JD, Kinter M and Hazen SL: Apolipoprotein A-I is a selective target for myeloperoxidase-catalyzed oxidation and functional impairment in subjects with cardiovascular disease. J Clin Invest 114: 529-541, 2004.
10. Francis GA: High density lipoprotein oxidation: *in vitro* susceptibility and potential *in vivo* consequences. Biochim Biophys Acta 1483: 217-235, 2000.
11. Thomas MJ, Chen Q, Zabalawi M, Anderson R, Wilson M, Weinberg R, Sorci-Thomas MG and Rudel LL: Is the oxidation of high-density lipoprotein lipids different than the oxidation of low-density lipoprotein lipids? Biochemistry 40: 1719-1724, 2001.
12. Marsche G, Heller R, Fauler G, Kovacevic A, Nuszkowski A, Graier W, Sattler W and Malle E: 2-Chlorohexadecanal derived from hypochlorite-modified high-density lipoprotein-associated plasmalogen is a natural inhibitor of endothelial nitric oxide biosynthesis. Arterioscler Thromb Vasc Biol 24: 2302-2306, 2004.
13. Norata GD, Pellegatta F, Hamsten A, Catapano AL and Eriksson P: Effects of HDL3 on the expression of matrix-degrading proteases in human endothelial cells. Int J Mol Med 12: 73-78, 2003.
14. Norata GD, Banfi C, Pirillo A, Tremoli E, Hamsten A, Catapano AL and Eriksson P: Oxidised-HDL3 induces the expression of PAI-1 in human endothelial cells. Role of p38MAPK activation and mRNA stabilization. Br J Haematol 127: 97-104, 2004.
15. Norata GD, Callegari E, Marchesi M, Chiesa G, Eriksson P and Catapano AL: High-density lipoproteins induce transforming growth factor-beta2 expression in endothelial cells. Circulation 111: 2805-2811, 2005.
16. Norata GD, Pirillo A, Callegari E, Hamsten A, Catapano AL and Eriksson P: Gene expression and intracellular pathways involved in endothelial dysfunction induced by VLDL and oxidised VLDL. Cardiovasc Res 59: 169-180, 2003.
17. Norata GD, Bjork H, Hamsten A, Catapano AL and Eriksson P: High-density lipoprotein subfraction 3 decreases ADAMTS-1 expression induced by lipopolysaccharide and tumor necrosis factor-alpha in human endothelial cells. Matrix Biol 22: 557-560, 2004.
18. Norata GD, Pirillo A, Pellegatta F, Inoue H and Catapano AL: Native LDL and oxidized LDL modulate cyclooxygenase-2 expression in HUVECs through a p38-MAPK, NF-kappaB, CRE dependent pathway and affect PGE2 synthesis. Int J Mol Med 14: 353-359, 2004.
19. Pirillo A, Norata GD, Zanelli T and Catapano AL: Over-expression of inducible heat shock protein 70 in Cos-1 cells fails to protect from cytotoxicity of oxidized ldls. Arterioscler Thromb Vasc Biol 21: 348-354, 2001.
20. Baez JM, Barbour SE and Cohen DE: Phosphatidylcholine transfer protein promotes apolipoprotein A-I-mediated lipid efflux in Chinese hamster ovary cells. J Biol Chem 277: 6198-6206, 2002.
21. Nagano Y, Arai H and Kita T: High density lipoprotein loses its effect to stimulate efflux of cholesterol from foam cells after oxidative modification. Proc Natl Acad Sci USA 88: 6457-6461, 1991.
22. Salmon S, Santus R, Maziere JC, Aubailly M and Haigle J: Modified apolipoprotein pattern after irradiation of human high-density lipoproteins by ultraviolet B. Biochim Biophys Acta 1128: 167-173, 1992.
23. Tsumura M, Kinouchi T, Ono S, Nakajima T and Komoda T: Serum lipid metabolism abnormalities and change in lipoprotein contents in patients with advanced-stage renal disease. Clin Chim Acta 314: 27-37, 2001.
24. Chin JH, Azhar S and Hoffman BB: Inactivation of endothelial derived relaxing factor by oxidized lipoproteins. J Clin Invest 89: 10-18, 1992.
25. Nuszkowski A, Grabner R, Marsche G, Unbehaun A, Malle E and Heller R: Hypochlorite-modified low density lipoprotein inhibits nitric oxide synthesis in endothelial cells via an intracellular dislocalization of endothelial nitric-oxide synthase. J Biol Chem 276: 14212-14221, 2001.
26. Matsunaga T, Hokari S, Koyama I, Harada T and Komoda T: NF-kappa B activation in endothelial cells treated with oxidized high-density lipoprotein. Biochem Biophys Res Commun 303: 313-319, 2003.
27. Linton MF and Fazio S: Cyclooxygenase-2 and inflammation in atherosclerosis. Curr Opin Pharmacol 4: 116-123, 2004.
28. Sheu ML, Chao KF, Sung YJ, Lin WW, Lin-Shiau SY and Liu SH: Activation of phosphoinositide 3-kinase in response to inflammation and nitric oxide leads to the up-regulation of cyclooxygenase-2 expression and subsequent cell proliferation in mesangial cells. Cell Signal 17: 975-984, 2005.
29. Yamamoto K, Arakawa T, Ueda N and Yamamoto S: Transcriptional roles of nuclear factor kappa B and nuclear factor-interleukin-6 in the tumor necrosis factor alpha-dependent induction of cyclooxygenase-2 in MC3T3-E1 cells. J Biol Chem 270: 31315-31320, 1995.
30. Schonbeck U, Sukhova GK, Graber P, Coulter S and Libby P: Augmented expression of cyclooxygenase-2 in human atherosclerotic lesions. Am J Pathol 155: 1281-1291, 1999.
31. Cipollone F, Prontera C, Pini B, Marini M, Fazia M, DeCesare D, Iezzi A, Ucchino S, Boccoli G, Saba V, Chiarelli F, Cuccurullo F and Mezzetti A: Overexpression of functionally coupled cyclooxygenase-2 and prostaglandin E synthase in symptomatic atherosclerotic plaques as a basis of prostaglandin E(2)-dependent plaque instability. Circulation 104: 921-927, 2001.
32. Topper JN, Cai J, Falb D and Gimbrone MA Jr: Identification of vascular endothelial genes differentially responsive to fluid mechanical stimuli: cyclooxygenase-2, manganese superoxide dismutase, and endothelial cell nitric oxide synthase are selectively up-regulated by steady laminar shear stress. Proc Natl Acad Sci USA 93: 10417-10422, 1996.
33. Vane JR and Botting RM: Pharmacodynamic profile of prostacyclin. Am J Cardiol 75: 3A-10A, 1995.

Cox-2 Is Regulated by Toll-Like Receptor-4 (TLR4) Signaling: Role in Proliferation and Apoptosis in the Intestine

MASAYUKI FUKATA,* ANLI CHEN,* ARIELLE KLEPPER,* SUNEETA KRISHNAREDDY,* ARUNAN S. VAMADEVAN,* LISA S. THOMAS,‡ RULIANG XU,§ HIROYASU INOUE,‖ MOSHE ARDITI,¶ ANDREW J. DANNENBERG,# and MARIA T. ABREU*

*Inflammatory Bowel Disease Center, Division of Gastroenterology, §Department of Medicine, Department of Pathology Mount Sinai School of Medicine, New York, New York; ¶Division of Pediatric Infectious Diseases, Department of Pediatrics, Steven Spielberg Pediatric Research Center, and ‡Inflammatory Bowel Disease Center, Burns and Allen Research Institute, Cedars-Sinai Medical Center, Los Angeles, California; ‖Department of Food Science and Nutrition, Faculty of Human Life and Environment, Nara Women's University, Nara, Japan; and #Department of Medicine, Division of Gastroenterology and Hepatology, New York Presbyterian Hospital and Weill Medical College of Cornell University, New York, New York

Background & Aims: We recently showed that mice deficient in Toll-like receptor 4 (TLR4) or its adapter molecule MyD88 have increased signs of colitis compared with wild-type (WT) mice after dextran sodium sulfate (DSS)-induced injury. We wished to test the hypothesis that cyclooxygenase 2 (Cox-2)–derived prostaglandin E_2 (PGE_2) is important in TLR4-related mucosal repair. **Methods:** Cox-2 expression was analyzed by real-time polymerase chain reaction, immunohistochemistry, Western blotting, and luciferase reporter constructs. Small interfering RNA was used to inhibit expression of MyD88. TLR4−/− or WT mice were given 2.5% DSS for 7 days. Proliferation and apoptosis were assessed using bromodeoxyuridine staining and terminal deoxynucleotidyl transferase–mediated deoxyuridine triphosphate nick-end labeling assays, respectively. PGE_2 was given orally to DSS-treated mice. **Results:** Intestinal epithelial cell lines up-regulated Cox-2 expression in a TLR4- and MyD88-dependent fashion. Lipopolysaccharide-mediated stimulation of PGE_2 production was blocked by a selective Cox-2 inhibitor or small interfering RNA against MyD88. After DSS injury, Cox-2 expression increased only in WT mice. TLR4−/− mice have significantly reduced proliferation and increased apoptosis after DSS injury compared with WT mice. PGE_2 supplementation of TLR4−/− mice resulted in improvement in clinical signs of colitis and restoration of proliferation and apoptosis to WT values. The mechanism for improved epithelial repair may be through PGE_2-dependent activation of the epidermal growth factor receptor. **Conclusions:** We describe an important link between TLR4 signaling and Cox-2 expression in the gut. TLR4 and MyD88 signaling are required for optimal proliferation and protection against apoptosis in the injured intestine. Although TLR4 signaling is beneficial in the short term, chronic signaling through TLR4 may lower the threshold for colitis-associated cancer.

The intestinal mucosa coexists with a high density of luminal bacteria and pathogen-associated molecular patterns. Indeed, the genetic program of the epithelium is shaped by the presence of bacteria. Compared with germ-free animals, colonization with a single species of gut commensal, *Bacteroides thetaiotaomicron*, results in the expression of genes that enhance barrier fortification and nutrient transport.[1] Early and now more recent studies have shown that germ-free animals have reduced intestinal epithelial cell proliferation compared with colonized mice.[2,3] Finally, germ-free mice are more susceptible to bleeding and death after dextran sodium sulfate (DSS)-induced colitis.[4] These data suggest a link between luminal bacteria and intestinal epithelial repair. Despite the beneficial role of bacteria in the normal function of the intestine, bacteria have been implicated in the pathogenesis of inflammatory bowel diseases (IBDs).[5,6] These disorders are characterized by chronic relapsing intestinal inflammation in the absence of a specific pathogen.

We became interested in the role of Toll-like receptor (TLR) signaling in the intestine as a means to better understand the relationship between epithelial function and bacteria during inflammatory states. TLRs are pattern-recognition receptors expressed by immune and nonimmune cells that signal in response to pathogen-associated molecular patterns expressed by microbes.[7] TLR signaling provides a rapid response against pathogens. Individual or pairs of TLRs recognize distinct pathogen-associated molecular patterns. For example, TLR4 is required for an immune response to lipopolysaccharide (LPS)[8,9] whereas TLR2 in combination with TLR1 recognizes lipoteichoic acid.[10] Most TLR molecules signal through the adapter molecule MyD88 to interleukin-1–receptor–associated kinase and Traf6 to transforming growth factor-β–activated kinase 1, resulting in activation of mitogen activated protein kinases and nuclear translocation of nuclear factor κB.[11]

Several lines of evidence support a role for TLR signaling in intestinal homeostasis. In vitro, TLR ligands induce fortification of intestinal barrier function through redistribution of the tight junction protein Zonula Occludens-1 (ZO-1)[12] and increase expression of β-defensin 2.[13] We and others have used an acute model of colitis to address the function of TLR4 in the setting of epithelial injury and inflammation. Administration of DSS to animals genetically deficient in TLR4 or MyD88 results in greater toxicity manifested by increased rectal bleeding, weight loss, and mortality compared with wild-type (WT) littermates.[14–16] We also have found that animals deficient in

Abbreviations used in this paper: BrdU, bromodeoxyuridine; Cox, cyclooxygenase; DSS, dextran sodium sulfate; EGFR, epidermal growth factor receptor; EIA, enzyme immunoassay; LPS, lipopolysaccharide; PCR, polymerase chain reaction; PGN, peptidoglycan; SD, standard deviation; siRNA, small interfering RNA; TLR, Toll-like receptor; TUNEL, terminal deoxynucleotidyl transferase–mediated deoxyuridine triphosphate nick-end labeling; WT, wild-type; ZO-1, Zonula Occludens-1.

0016-5085/06/$32.00
doi:10.1053/j.gastro.2006.06.017

TLR4 or MyD88 have decreased neutrophil recruitment to the intestine owing to defective expression of chemokines and they experience bacterial translocation to mesenteric lymph nodes.[15] At least part of the reason for the increased bleeding and weight loss may be owing to decreased intestinal epithelial cell proliferation in TLR4 or MyD88 knock-out mice.[3,14,15] This series of observations have led to the conclusion that recognition of luminal bacteria through the intestinal expression of TLRs is important for intestinal homeostasis.

The relationship between epithelial repair and inflammation is complex. An important mediator of both inflammation and repair in the intestine is cyclooxygenase (Cox)-2. Cox-1 and Cox-2 synthesize prostaglandins (PGs) from arachidonic acid.[17] Although intestinal epithelial cells express Cox-1 constitutively, Cox-2 is induced by inflammatory mediators. Cox-2–dependent PGE_2 production is critical for epithelial repair in the intestine in a variety of contexts. In the setting of IBD, increased Cox-2 and PGE_2 have been implicated in the development of colitis-associated cancers.[18,19] We recently showed that microsomal PGE synthase-1, the enzyme that catalyzes the conversion of PGH_2 to PGE_2, is increased in IBD mucosa[18] whereas 15-hydroxyprostaglandin dehydrogenase, the enzyme responsible for catabolism of PGE_2, is reduced in the inflamed mucosa of IBD.[19] This combination results in overall increases in mucosal PGE_2, and the potential for enhanced carcinogenesis in the setting of inflammation.

We wished to better understand the cellular and molecular mechanisms by which TLR4 signaling is involved in intestinal homeostasis. Studies performed before the identification of TLR4 found that systemic administration of LPS protected animals from radiation-induced injury in the gut characterized by apoptosis of intestinal stem cells.[20,21] The mechanism for the LPS-induced radioprotection was found to be induction of Cox-2 and PGE_2 production.[21] In addition, DSS administration to Cox-2 knock-out mice results in a phenotype reminiscent of that seen in TLR4−/− mice, namely increased bleeding and increased mortality.[22]

In the current study, we test the hypothesis that Cox-2–derived PGE_2 is important in TLR4-dependent mucosal homeostasis. Our data show that TLR4-deficient mice fail to up-regulate Cox-2 expression in response to epithelial injury. Both intestinal epithelial cells and lamina propria macrophages express Cox-2 in a TLR4- and MyD88-dependent fashion. PGE_2 is decreased in the mucosa of TLR4−/− mice after DSS injury. Oral supplementation with PGE_2 results in increased intestinal epithelial cell proliferation and decreased apoptosis in DSS-treated TLR4−/− mice. At least part of the mechanism for TLR4-dependent mucosal healing involves activation of epidermal growth factor receptor (EGFR) signaling. The results of our studies shed an important light on the previously unrecognized role of TLR signaling in the regulation of Cox-2 in the gut.

Materials and Methods

Mice and Interventions

TLR4−/− mice and MyD88−/− mice were purchased from Oriental Bio Service, Inc. (Kyoto, Japan). All knock-out mice used were back-crossed to C57Bl/6 mice more than 8 times. C57Bl/6 mice were obtained from Jackson Laboratory as controls (Bar Harbor, ME). Seven- to 10-week-old sex-matched mice were given 2.5% DSS (molecular weight, 36–50 kilodaltons; ICN, Aurora, OH) in their drinking water and were killed at the end of 7 days of DSS treatment. For recovery studies, DSS was administered for the first 7 days as indicated, and then DSS was removed from the drinking water and mice were killed 7 days after the cessation of DSS treatment. PGE_2 (Cayman, Ann Arbor, MI) was diluted from the ethanol stock (10 $\mu g/\mu L$) in phosphate-buffered saline (PBS) and 200 μg in 150 μL was given twice daily by gavage feeding, starting 3 hours before first DSS administration as described previously.[23,24] Control mice were given PBS including the same dilution of ethanol. All experiments were performed according to the Mount Sinai School of Medicine Animal Experimental Ethics Committee guidelines.

Assessment of Colitis Activity

Body weight was assessed at baseline and every day for the duration of the experiment. Weight change was calculated as the percentage change in weight compared with baseline. Fecal blood was tested daily using Hemoccult cards (Beckman Coulter, Inc., Fullerton, CA) and graded as follows: 0 = no blood, 1 = trace blood, 2 = positive, and 4 = gross blood. Mice were euthanized by CO_2 followed by cervical dislocation. The cecum was removed and the remainder of the colon was divided into proximal and distal halves. Tissue was fixed in 10% buffered formalin, paraffin-embedded, sectioned, and stained with H&E. Histologic assessment was performed by a pathologist blinded to the mouse genotype and treatment. Histologic score was a combined score of acute inflammatory cell infiltrate (0–4), chronic inflammatory cell infiltrate (0–3), and crypt damage (0–4).[25–27] Specifically, the crypt damage was scored in the following manner. A score of 0 was given to an intact crypt, 1 = loss of the basal one third of the crypt; 2 = loss of the basal two thirds of the crypt; 3 = entire loss of crypt; and 4 = loss of crypt and surface epithelium.[26] Because the injury from DSS is patchy, 2 slides from each section of the colon were assessed per mouse and at least 3 areas on each slide were examined.

Cell Lines and Reagents

Human intestinal cell lines SW480 and T84 (1×10^6 cells/well) and mouse macrophage cell line RAW264.7 (1.5×10^6 cells/well) (American Type Culture Collection, Manassas, VA) were maintained in Dulbecco's modified Eagle medium supplemented with 10% heat-inactivated fetal calf serum, 2 mmol/L L-glutamine, 5% penicillin/streptomycin, and were incubated in 6-well plates overnight at 37°C in a 5% CO_2 humidified incubator. Cells were incubated with phenol-water–extracted *Escherichia coli* K235 LPS (Sigma, St. Louis, MO), synthetic bacterial lipoprotein (Pam3CSK4) (InvivoGen, San Diego, CA), peptidoglycan (PGN) (InvivoGen), or vehicle for the indicated periods of time. Cox inhibitor NS398 and indomethacin (Sigma) were added at the same time as LPS. AG1478, an EGFR tyrosine kinase inhibitor, was added 30 minutes before LPS stimulation. Recombinant human EGF (R&D Systems, Minneapolis, MN) was used as a control.

Real-Time Polymerase Chain Reaction

Total RNA was isolated by using RNA Bee (Tel-Test, Inc., Friendwood, TX) according to the manufacturer's instructions. A total of 1 μg RNA was used as the template for single-strand complementary DNA (cDNA) synthesis using the Transcriptor First Strand cDNA Synthesis Kit (Roche, India-

Table 1. Sequence of the Primers and Probes Used

Gene	Forward primer	Reverse primer	Probe
Human			
Cox-2	GCA CGT CCA GGA ACT CCT CA	GGG GTA GGC TTT GCT GTC TG	CCT TCA GCT CCA CAG CCA GAC GCC
MyD88	CTC CTC CAC ATC CTC CCT TCC	CCG CAC GTT CAA GAA CAG AGA	CGC CGC ACT CGC ATG TTG AGA GCA
β-actin	GAC TGA GTC TTG CTC TGT CGG	GGC ATG ATG GCT TAC GCC TAT A	AGC GAC TCC TGT GCC TCA GCC TCC
Mouse			
Cox-1	AAG GAG TCT CTC GCT CTG GTT T	TCT CAG GGA TGG TAC AGT TGG G	TGC TCC TGC TGC TGC CGC CGA
Cox-2	ATC CTG CCA GCT CCA CCG	TGG TCA AAT CCT GTG CTC ATA CAT	ACT GCC ACC TCC GCT GCC ACC T
β-actin	ATG ACC CAG ATC ATG TTT GA	TAC GAC CAG AGG CAT ACA	CGT AGC CAT CCA GGC TGT GC

NOTE. Sequences are listed in 5′ to 3′ direction.

napolis, IN) according to the manufacturer's instructions. Quantitative real-time polymerase chain reaction (PCR) was performed for Cox-2, MyD88, Cox-1, and β-actin using TaqMan (Applied Biosystems, Foster City, CA) probes (Table 1). All TaqMan probes and primers were designed using Beacon Designer 3.0 (Premier Biosoft International, Palo Alto, CA) (Table 1). The cDNA was amplified using TaqMan universal PCR Master Mix (Roche) on the ABI Prism 7900HT sequence detection system (Applied Biosystems), programmed for 95°C for 10 minutes, then 40 cycles of 95°C for 15 seconds, and 60°C for 1 minute. The amplification results were analyzed using SDS 2.2.1 software (Applied Biosystems) and the genes of interest were normalized to the corresponding β-actin results. Data were expressed as fold induction relative to the lowest one.

RNA Interference

SW480 cells were plated at a density of 1.5×10^5 cells/well in 12-well plates 24 hours before the first transfection. MyD88 small interfering RNA (siRNA) oligonucleotide corresponding to the sequence (GCUCAUCGAAAAGAGGUGCtt) was purchased from Ambion (Austin, TX) and 50 nmol/L of siRNA were transfected twice every 24 hours with X-trim gene siRNA transfection reagent (Roche) as per the manufacturer's instructions. Forty-eight hours after the first transfection, cells were stimulated with LPS for the indicated period of time. siRNA (50 nmol/L), which has no significant homology to any known gene sequences from mouse, rat, or human being, and siRNA against glycerol dehyde-3-phosphate dehydrogenase were used as negative controls (Ambion).

Western Blot Analysis

Whole-cell lysates were prepared from colonic tissue samples or SW480 cells after treatment with different stimuli using a lysis buffer containing 50 mmol/L Tris HCl, 50 mmol/L NaF, 1% Triton X-100, 2 mmol/L ethylenediaminetetraacetic acid [EDTA], and 100 mmol/L NaCl, with a proteinase inhibitor cocktail (Calbiochem, San Diego, CA). The protein concentration was determined by the Bradford method using Bio-Rad Protein Assay Dye and SmartSpec 3000 (Bio-Rad Laboratories, Hercules, CA). A total of 25 μg of the lysates were subjected to 8% or 10% sodium dodecyl sulfate-polyacrylamide gel electrophoresis and transferred to Immobilon-P membranes (Millipore Corporation, Bedford, MA). The membrane was blocked in 5% skim milk and was immunoblotted with the primary antibodies for 1 hour, followed by horseradish-peroxidase-conjugated secondary antibodies rabbit anti-mouse or goat anti-rabbit IgG (Zymed Laboratories, South San Francisco, CA). The membrane was exposed on radiographic film using an enhanced chemiluminescent substrate SuperSignal West Pico Trial Kit (Pierce Biotechnology, Rockford, IL). Antibodies specific for murine or human Cox-2 were purchased from Cayman. Anti-MyD88 antibody (HFL-296) was purchased from Santa Cruz Biotechnology (Santa Cruz, CA).

Immunofluorescent and Immunohistochemical Studies

Cecum, proximal, and distal colon were freshly isolated and frozen in Optimal Cutting Temperature (OCT; Sakura Finetek, Torrance, CA) or fixed in 10% neutral buffered formalin and embedded in paraffin wax. Part of the samples were fixed with modified Bouin's fixative consisting of 0.5% paraformaldehyde acetate and 15% (vol/vol) of saturated picric acid in 0.1 mol/L PBS pH 7.0. Frozen sections prefixed by modified Bouin's fixation were incubated in 10% normal goat serum for 1 hour and stained with antimurine Cox-2 antibody (1:200; Cayman) overnight at 4°C, followed by TRITC (tetramethyl rhodamine isothiocyanate)-conjugated anti-rabbit IgG (1:200, Zymed Laboratories) for 1 hour at room temperature. The specificity of staining was confirmed using Cox-2 blocking peptide (Cayman) according to the manufacturer's instructions or using rabbit isotype control antibody instead of the primary antibody (Zymed Laboratories).

Double-immunofluorescent staining of CD68 and Cox-2 was performed using prefixed OCT sections. Sections were incubated with 0.1% trypsin (Sigma) $CaCl_2$ dissolved in 0.05 mol/L Tris-Hcl pH 7.6 for 15 minutes at 37°C. Subsequently sections were blocked in 5% skim milk for 1 hour and then incubated with the rat anti-CD68 antibody (1:20, MCA1957S; Serotec Ltd., Raleigh, NC) overnight at 4°C. After washing in PBS, sections were incubated with TRITC-conjugated rabbit anti-rat IgG (1:200; Sigma) for 1 hour at room temperature. Then sections were re-incubated with 5% skim milk followed by Cox-2 staining as described previously using fluorescein isothiocyanate-conjugated goat anti-rabbit IgG (1:200, Sigma).

Phospho-specific EGFR staining was performed using OCT sections. After blocking with 5% milk, sections were incubated with anti-phospho-EGFR antibody (1:200; Santa Cruz) overnight at 4°C. Secondary antibody (fluorescein isothiocyanate-conjugated anti-goat IgG; Sigma) was used at a dilution of 1:200. As a negative control, primary antibody was omitted and tissue was stained with secondary antibody alone. To quantify the expression level of phospho EGFR, staining intensity was analyzed using MetaMorph software (Universal Imaging Corporation, Downingtown, PA). Epithelial cells were selected randomly and the average pixel intensities from 10 areas of gated cells per slide were analyzed to compare the expression levels of phospho EGFR.

Staining of SW480 was performed using 4-chamber slides (Nalgene Nunc International, Rochester, NY), in which cells were

seeded at a density of 1×10^5 cells/well on the day before the experiment. Cells were stained with goat anti-EGFR or anti-phospho-EGFR antibodies (dilution of 1:300) after methanol fixation and preparation with 0.5% Triton X-100. Nonspecific binding was blocked with 5% skim milk. Fluorescein isothiocyanate-conjugated goat anti-rabbit or sheep anti-mouse IgG (1:200; Sigma) was used as a secondary antibody.

SW480 and double-stained tissue slides were examined using a Leica TCS-SP (UV) confocal microscope (Leica, Bannockburn, IL). Four thin optical sections through the x-y axis were acquired. Other slides were viewed on a Nikon eclipse E600 immunofluorescence microscope (Nikon, Melville, NY) and photographs were taken with a digital camera using Spot Advanced software program (Diagnostic Instruments Inc., Sterling Heights, MI).

Assessment of Proliferation and Apoptosis

The number of proliferating cells was detected by immunoperoxidase staining for the thymidine analog bromodeoxyuridine (BrdU). At 1.5 hours before death, mice were injected intraperitoneally with 5-bromo-2'-deoxyuridine (Sigma) at a concentration of 100 mg/kg. Sections (4 μm) of paraffin-embedded colonic tissue were deparaffinized and incubated with 3% H_2O_2 in methanol for 15 minutes. Sections were incubated with 2 N HCl for 1 hour, washed in PBS, and then incubated in 0.1% trypsin for 15 minutes at 37°C. Sections were stained for BrdU incorporation using a BrdU staining kit (Zymed Laboratories Inc.) according to the manufacturer's instructions. The number of BrdU-positive cells per well-oriented crypt was calculated in every 3 crypts for each colon segment at high magnification under light microscopy.

Apoptotic cells in the colonic epithelial cells were detected using the terminal deoxynucleotidyl transferase-mediated deoxyuridine triphosphate nick-end labeling (TUNEL) assay (ApopTaq *In Situ* Apoptosis Detection Kit; Chemicon, Temecula, CA), following the manufacturer's instruction. Briefly, paraffin sections were prepared with proteinase K (20 μg/mL). After equilibration with terminal deoxynucleotidyl transferase buffer, sections were reacted with terminal deoxynucleotidyl transferase enzyme for 1 hour at 37°C. Digoxigenin-labeled free 3'-OH end of DNA was detected by anti-digoxigenin-rhodamine conjugate. Sections were counterstained with 4',6-diamidino-2-phenylindole. The apoptotic cells were counted as follows: 300 epithelial cells were counted per high-power field and scored for apoptosis; a total of 3 fields were counted per section of mouse colon (ie, cecum, proximal, and distal colon). Three mouse colons were counted per condition. The apoptotic index was determined by the ratio of TUNEL-positive nuclei to 100 total nuclei in the epithelial cells counted. The areas of necrosis such as in an ulcer bed were identified by examining the corresponding H&E slides and were excluded from counting for apoptotic cells as previously described.[28]

Transient Gene Expression and Reporter Gene Assays

SW480 cells were plated in 12-well plates at a density of 1.5×10^5 cells/well. Cells were transfected the following day with FuGENE 6 transfection reagent (Roche) as per the manufacturer's instructions. Reporter genes for pRL-TK (0.05 μg), Cox-2 promoter-luciferase constructs (phPES2 −1432/+59: 0.3 μg),[29,30] which were provided by Dr Inoue (Nara Women's University, Nara city, Japan), pGL3 basic empty vector (0.3 μg) were cotransfected as indicated in Figure 1. After overnight transfection, cells were stimulated with LPS (5 μg/mL) for 4 hours. Cells then were lysed and firefly luciferase activity was measured with a Dual-Luciferase Reporter Assay (Promega, San Luis Obispo, CA). Luciferase measurements were normalized to the relative light units from Renilla luciferase from pRL-KT. For experiments in which the Cox-2 promoter and siRNA against MyD88 were used, the siRNA (50 nmol/L) was transfected on day 1, then 24 hours later the promoter construct (0.3 μg) and the siRNA (50 nmol/L) were transfected (day 2). Cells then were stimulated and harvested for the indicated times. Data are reported as fold-induction over cells transfected with a control empty vector.

Measurement of PGE_2

Production of PGE_2 in the tissue culture supernatant was determined using a monoclonal enzyme immunoassay (EIA) kit (Cayman) according to the manufacturer's instructions and Morteau et al.[22] Briefly, colonic samples from TLR4−/− and WT mice were washed in cold PBS containing penicillin, streptomycin, and fungizone (100 U/mL each). A total of 100 mg of tissue fragments from each part of the colon were cultured for 24 hours in 12-well flat-bottom plates in serum-free RPMI 1640 supplemented with penicillin, streptomycin, and fungizone (100 U/mL each). Culture supernatants were harvested for PGE_2 measurement.

Flow Cytometry

Intracellular phospho-specific flow cytometry was used to quantify the effect of LPS on EGFR phosphorylation as previously described.[31,32] Briefly, LPS-stimulated or LPS-unstimulated SW480 cells were fixed in 2% paraformaldehyde at room temperature for 10 minutes. After washing with wash buffer (0.5% bovine serum albumin and 2 mmol/L EDTA in PBS), cells were permeabilized in 0.1% Triton X-100 for 5 minutes. Then cells were stained with phospho EGFR (1:500) for 30 minutes at room temperature. After 3 washes with the wash buffer, cells were incubated with TRITC-conjugated sheep anti-mouse IgG (Zymed Laboratories Inc.) for 20 minutes on ice. After washing with wash buffer, cells were filtered and analyzed by FACScan (Becton Dickinson, Franklin Lakes, NJ). Fluorescence intensity was normalized using isotype control antibody.

Cell Proliferation Assay

SW480 cells (5×10^4 cells/well) were cultured in 96-well plates in the absence or presence of AG1478 (10 μmol/L) in low serum condition (1% fetal calf serum), and stimulated with LPS (2 μg/mL). After 12 or 24 hours of stimulation, cell proliferation was analyzed using CellTiter 96 aqueous nonradioactive cell proliferation assay kit (Promega, Madison, WI). Cell proliferation was detected by measurement of formazan product in each well at the absorbance of 490 nm after incubation with tetrazolium/phenazine methosulfate for 1 hour at 37°C. The cell proliferation index was calculated as a percentage of the absorbance in relation to the untreated control cells.

Statistical Analysis

Calculation of the Student *t* test and standard deviation (SD) were performed using the statistics package within Microsoft Excel (Microsoft, Redmond, WA). Standard error was

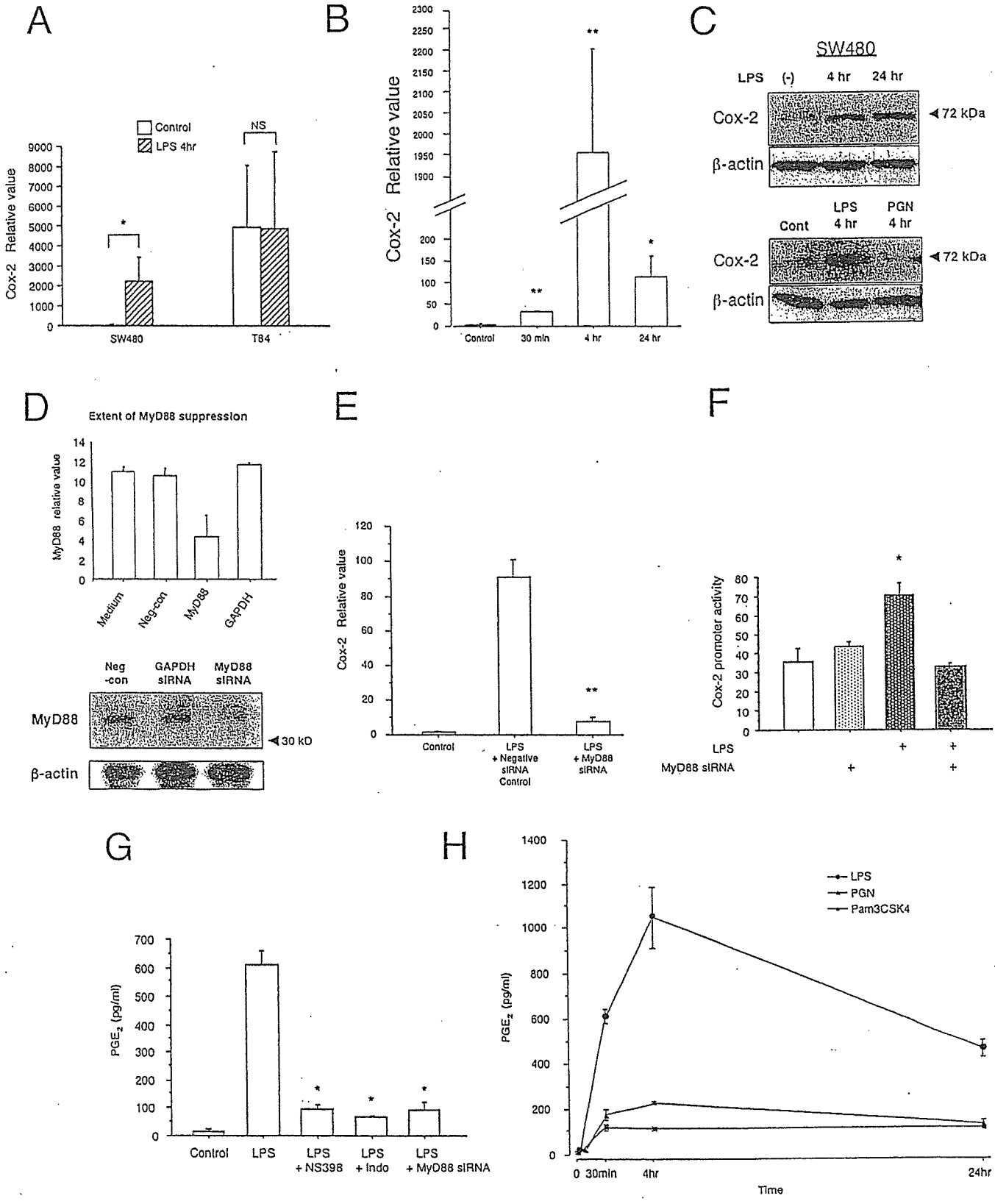
A
Control
LPS 4hr
NS
Cox-2 Relative value
SW480
T84
B
Cox-2 Relative value
Control
30 min
4 hr
24 hr
C
SW480
LPS (-) 4 hr 24 hr
Cox-2
β-actin
72 kDa
Cont
LPS 4 hr
PGN 4 hr
D
Extent of MyD88 suppression
MyD88 relative value
Medium
Neg-con
MyD88
GAPDH
Neg -con
GAPDH siRNA
MyD88 siRNA
30 kD
E
Cox-2 Relative value
Control
LPS + Negative siRNA Control
LPS + MyD88 siRNA
F
Cox-2 promoter activity
LPS
MyD88 siRNA
G
PGE2 (pg/ml)
Control
LPS
LPS + NS398
LPS + Indo
LPS + MyD88 siRNA
H
PGE2 (pg/ml)
LPS
PGN
Pam3CSK4
0 30min 4hr 24hr
Time

calculated with Stat View (Abacus Concept, Berkeley, CA). *P* values less than .05 were considered significant.

Results

Cox-2 Expression and PGE_2 Production by Intestinal Epithelial Cells Is TLR4 and MyD88 Dependent

Previous studies have shown that TLR4 signaling is involved in regulating Cox-2 expression in RAW264.7 cells.[33] We hypothesized that TLR4 also was important for Cox-2 expression by intestinal epithelial cells. To address this question, we compared the effect of LPS on Cox-2 expression in a cell line that expresses TLR4 and activates nuclear factor κB in response to LPS (SW480) vs a cell line that does not express TLR4 and is LPS unresponsive (T84).[13,34] The baseline expression of Cox-2 differed in these neoplastic cell lines.[35] Only TLR4-responsive SW480 cells increased expression of Cox-2 in response to LPS (Figure 1*A*). Induction of Cox-2 proceeded with rapid kinetics occurring within 30 minutes of LPS stimulation and peaking at 4 hours (Figure 1*B*); protein expression for Cox-2 remained increased at 24 hours after LPS stimulation (Figure 1*C*). No induction of Cox-2 protein was seen after stimulation with PGN, a TLR2 ligand (Figure 1C, lower panel).

To clarify further whether LPS induction of Cox-2 requires MyD88, we transfected SW480 cells with siRNA against MyD88 or a control siRNA (Figure 1*D*). Only the siRNA specific for MyD88 inhibited LPS-mediated expression of Cox-2 RNA. Finally, we asked whether LPS could induce Cox-2 promoter activation and whether this also depended on MyD88. A full-length Cox-2 promoter–luciferase construct was transfected into cells in the presence or absence of siRNA against MyD88 (Figure 1*E*). LPS activated the Cox-2 promoter and this activation was blocked by MyD88 siRNA. We performed dose-ranging studies using the Cox-2 promoter–reporter gene and found no difference in induction of the reporter between 2 and 5 μg/mL of LPS (data not shown). Taken together, these data show that LPS can directly induce Cox-2 promoter activity, messenger RNA (mRNA) expression, and protein expression in a TLR4- and MyD88-dependent fashion in colonic epithelial cells.

Cox-2 metabolizes arachidonic acid released from the plasma membrane to generate prostanoids such as PGE_2. PGE_2 in turn mediates many of the biologic effects of Cox-2 in the intestinal epithelium.[36] LPS previously has been shown to stimulate PGE_2 production by intestinal epithelial cell lines,[37-39] although most studies have attributed the biologic effects of LPS in the gut to macrophages and other stromal cells.[40] We hypothesized that LPS-mediated induction of PGE_2 depended on MyD88 signaling. Our results show that LPS induces PGE_2 production by SW480 cells (Figure 1*F*). PGE_2 production could be blocked by expression of MyD88 siRNA to an extent that was similar to a selective Cox-2 inhibitor or a nonselective Cox inhibitor, indomethacin. By contrast, stimulation with the TLR2 ligands PGN and PamCysk3 induced very little less PGE_2, especially when compared with LPS (Figure 1*G*). These data suggest that LPS stimulation of TLR4 leads to Cox-2 expression and the production of PGE_2 by intestinal epithelial cells in vitro.

Figure 1. LPS induces Cox-2 expression in human intestinal epithelial cell lines in a TLR4- and MyD88-dependent fashion. (*A*) Cox-2 expression after stimulation with LPS (2 μg/mL) in T84 (LPS unresponsive) and SW480 (LPS responsive) human intestinal epithelial cell lines. TaqMan real-time PCR showed inducible Cox-2 expression stimulated by LPS in SW480 cells. LPS-unresponsive T84 cells showed no change in Cox-2 expression in response to LPS stimulation. Data are represented as mean ± SEM of relative values of expression in 3 individual experiments of triplicate samples (**P* < .05). (*B*) LPS-responsive SW480 cells were stimulated with LPS (2 μg/mL) for indicated times. TaqMan real-time PCR shows LPS-induced expression of Cox-2 mRNA with a peak at 4 hours of stimulation. Data are represented as mean ± SEM of relative values of expression in 3 individual experiments of triplicate samples (**P* < .05, ***P* < .001). (*C*) Western blot analysis of Cox-2 protein expression in SW480. Cells were stimulated with LPS for indicated periods in *top panel*. *Lower panel* shows stimulation of cells with LPS (2 μg/mL) or PGN (2 μg/mL). Blots of whole-cell lysates (25 μg/*lane*) were probed with Cox-2 antibody. Data are 1 of 3 representative experiments with similar results. β-actin was used as an internal control for protein loading. (*D*) Extent of MyD88 suppression by siRNA. SW480 cells were transfected transiently with siRNA against MyD88 or glycerol dehyde-3-phosphate dehydrogenase (GAPDH). Negative siRNA, which has no significant homology to any gene sequences, was applied as a control. The knock-down efficiency of siRNA against MyD88 was assessed by real-time PCR and Western blot. The siRNA decreased both MyD88 mRNA and protein expression. Negative siRNA and siRNA against GAPDH did not affect MyD88 mRNA or protein expression. (*E*) MyD88-dependent induction of Cox-2 in response to LPS. SW480 cells were stimulated with LPS (5 μg/mL) for 4 hours and cotransfected with either MyD88 siRNA or negative control siRNA. Untransfected control samples were not LPS treated. TaqMan real-time PCR showed LPS-induced expression of Cox-2 in negative control siRNA samples. This induction of Cox-2 by LPS was largely abolished in the cells in which MyD88 was blocked with siRNA, indicating a MyD88-dependent pathway. Data are represented as mean ± SEM of relative values of expression in 3 individual experiments of triplicate samples (***P* < .001). (*F*) LPS regulation of Cox-2 gene promoter activity. The intestinal epithelial cell line SW480 was cotransfected with the Cox-2 (−1432/+59) luciferase reporter construct, MyD88 siRNA, or the empty pGL3 vector control, together with an internal control pRL-KT (Renilla luciferase) plasmid. Cells were stimulated with LPS (5 μg/mL) for 4 hours. Reporter gene activation was significantly higher in cells stimulated with LPS than nonstimulated cells. MyD88 siRNA abrogated promoter activation in response to LPS. Data are represented as mean ± SEM of relative light units in 3 individual experiments with triplicate samples (**P* < .05). (*G*) LPS-induced PGE_2 production in the intestinal epithelial cell line SW480. Cells were stimulated with LPS (2 μg/mL) for 30 minutes. PGE_2 concentration in supernatant was measured by monoclonal EIA. LPS stimulation resulted in PGE_2 production within 30 minutes. MyD88 siRNA inhibited LPS-induced PGE_2 production, as did a selective Cox-2 inhibitor (NS398 5 μmol/L) or a Cox-1/Cox-2 inhibitor (indomethacin 5 μmol/L). Data are represented as mean ± SEM of 2 individual measurements of duplicate samples taken from 3 individual experiments (**P* < .05). (*H*) Effect of TLR2 ligands on production of PGE_2 compared with the TLR4 ligand LPS in the intestinal epithelial cell line SW480. SW480 was stimulated with a TLR4 ligand LPS (2 μg/mL), or TLR2 ligands PGN (2 μg/mL) or Pam3CSK4 (500 ng/mL) for indicated periods of time. The concentration of PGE_2 was examined by monoclonal EIA. There were significant differences in the stimulation of PGE_2 between LPS vs TLR2 ligands. Data are represented as the mean ± SD of triplicate samples taken from 2 individual experiments (*P* < .05, between LPS and PGN or Pam3CSK4 for each time period).

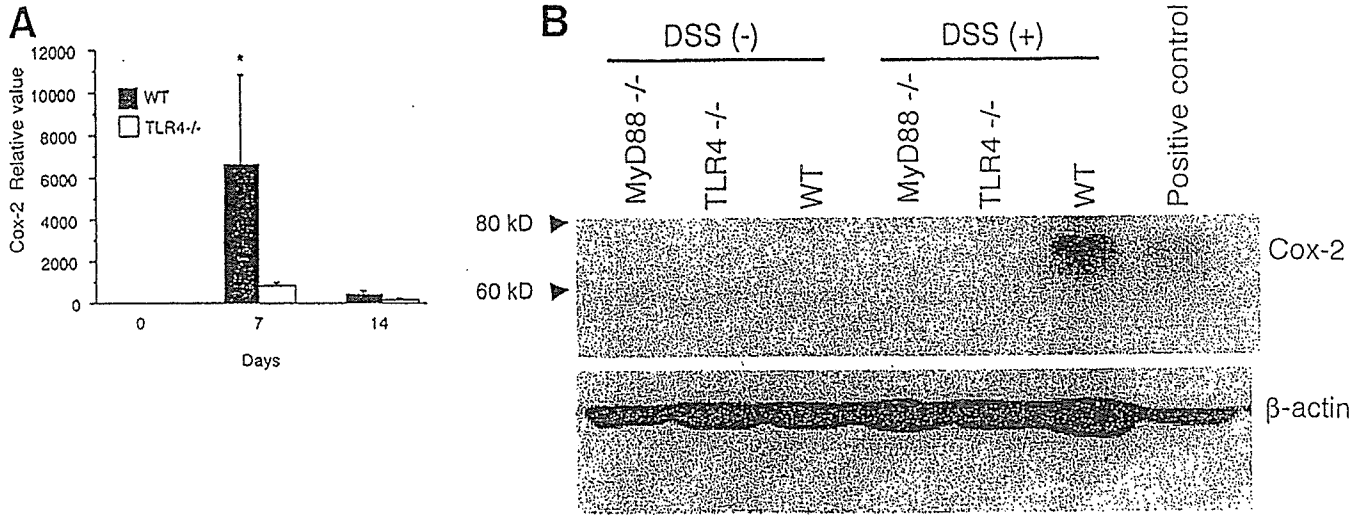
A
Cox-2 Relative value
12000
10000
8000
6000
4000
2000
0
WT
TLR4-/-
*
0
7
14
Days
B
DSS (-)
DSS (+)
MyD88 -/-
TLR4 -/-
WT
MyD88 -/-
TLR4 -/-
WT
Positive control
80 kD
60 kD
Cox-2
β-actin

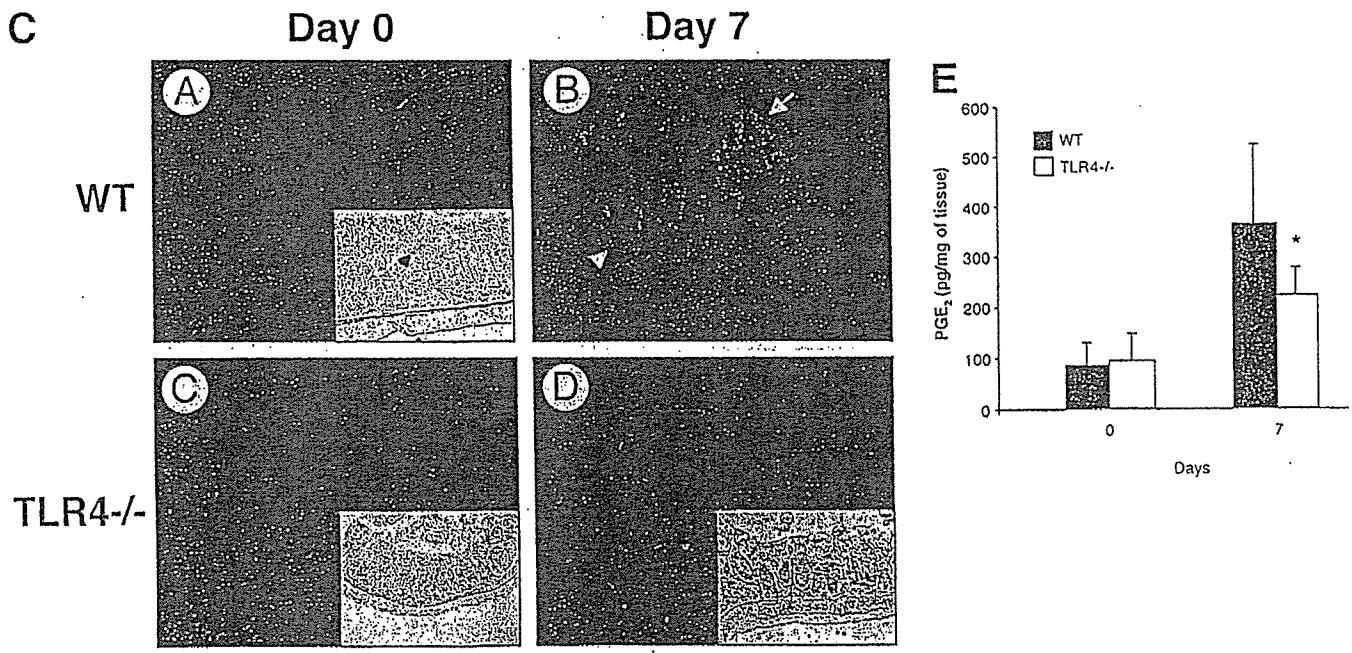
C
Day 0
Day 7
WT
TLR4-/-
A
B
C
D
E
PGE2 (pg/mg of tissue)
600
500
400
300
200
100
0
WT
TLR4-/-
*
0
7
Days

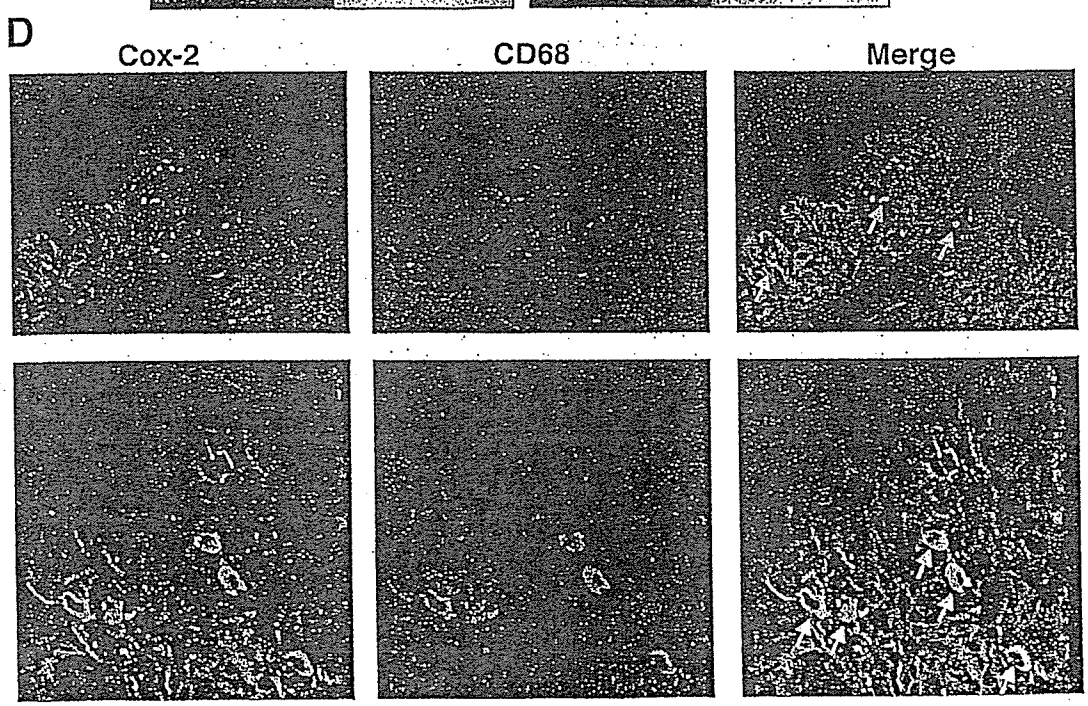
D
Cox-2
CD68
Merge

Cox-2 and PGE_2 Expression Are Decreased in TLR4-Deficient Mice After DSS-Induced Injury

Cox-2 expression is increased in human IBD and animal models of colitis including DSS.[22,41] Based on our in vitro findings, we hypothesized that TLR4 signaling was important for Cox-2 expression in the setting of DSS colitis. By using real-time PCR we found that Cox-2 expression is low in WT and TLR4−/− mice before DSS treatment (Figure 2*A*), whereas Cox-1 is expressed abundantly in both (data not shown). After induction of colitis, there is a dramatic increase in expression of Cox-2 in WT mice. This up-regulation is not seen in TLR4−/− mice. We confirmed protein expression of Cox-2 by Western blot analysis of tissue lysates (Figure 2*B*) and immunofluorescence (Figure 2*C*). Colonic tissue from WT mice or LPS-treated RAW cells expressed Cox-2, but little was present in TLR4−/− colon tissue. Immunofluorescent studies revealed both epithelial staining and lamina propria staining of Cox-2 in WT mice. To define the cell types expressing Cox-2 in the lamina propria of WT mice, we performed double staining with a macrophage marker CD68 and anti-Cox-2 antibody (Figure 2*D*). Most Cox-2–positive cells in the lamina propria were also CD68 positive, suggesting that lamina propria macrophages express Cox-2 in the inflamed colon. These data support a role for TLR4 regulation of Cox-2 expression in the intestine.

Given that mice that are deficient in TLR4 do not express Cox-2, we hypothesized that TLR4−/− mice would have decreased production of PGE_2. To test this hypothesis, we measured production of PGE_2 from colonic tissue using monoclonal EIA. Our data show that PGE_2 production by colonic tissues is reduced significantly in TLR4-deficient mice after DSS-induced injury (Figure 2*E*). PGE_2 production in TLR4−/− mice was decreased by 40% compared with WT mice after DSS colitis. These data suggest that at least one defect in TLR4−/− mice with respect to epithelial repair is reduced production of local PGE_2.

TLR4−/− Mice Have Decreased Proliferation and Increased Intestinal Epithelial Cell Apoptosis After DSS-Induced Colitis

Cox-2 knock-out mice show increased susceptibility to DSS colitis similar to what we have observed in TLR4−/− mice. We have previously described that TLR4−/− mice have decreased intestinal epithelial proliferation after acute DSS-induced injury.[15] Given our findings of decreased Cox-2 expression, we wished to examine the effect of TLR4 deficiency on baseline levels of proliferation, at the peak of injury, and 7 days after recovery (day 14). By using BrdU labeling of proliferating intestinal epithelial cells, we show that proliferation is similar in WT and TLR4−/− mice before DSS treatment (Figure 3*A* and 3*B*). After DSS-induced injury, WT mice have a large increase in proliferating cells that persists even a week after DSS is discontinued. By contrast, TLR4−/− mice have significantly fewer proliferating cells. By using computerized microscopic measurements, we found a significant decrease in crypt height in the injured TLR4−/− gut that can be appreciated in the photomicrographs (Figure 3*A*) (day 7: WT, 291 ± 48.2 μm; TLR4−/−, 214 ± 20.2 μm; $P < .0001$; day 14: WT, 257 ± 111 μm; TLR4−/−, 167 ± 35.1 μm; $P < .0001$). Importantly, crypt height is similar at baseline in WT and TLR4−/− mice, suggesting this defect in proliferation is only apparent in the setting of injury (day 0: WT, 244 ± 72.9 μm; TLR4−/−, 251 ± 49.5 μm; $P < .321$).

Colonic crypt height represents the balance of epithelial proliferation and apoptotic cell loss at the top of the crypts.[28,42] We reasoned, therefore, that TLR4−/− mice could have increased intestinal epithelial cell apoptosis in response to DSS injury. To address this question, we performed TUNEL staining on intestinal sections from DSS-treated TLR4−/− mice or their WT controls (Figure 3*C* and *D*). We found significantly more apoptotic cells per crypt in TLR4−/− intestine compared with controls. In general, the apoptotic cells were found at the tops of the colonic crypts. Similar findings were seen in MyD88−/− mice, suggesting this was an MyD88-dependent phenomenon (data not shown). An increased rate of apoptosis was not seen in the intestines of mice before DSS treatment. We conclude from these data that TLR4 is important for intestinal epithelial repair from injury by aiding in proliferation and protecting against apoptosis.

PGE_2 Restores Proliferation and Protects Against Apoptosis in TLR4−/− Mice

We have shown previously that TLR4 is required for induction of Cox-2 and PGE_2 during DSS-induced injury. We hypothesized that the decrease in PGE_2 production in TLR4−/− mice was responsible for the observed phenotype,

Figure 2. Cox-2 expression is decreased in TLR4−/− mice after DSS-induced colitis. (*A*) TaqMan real-time PCR showed up-regulation of Cox-2 expression in the colon of WT mice but not in TLR4−/− mice after 7 days of DSS treatment (n = 3 for each group on day 0, n = 12 for the other groups). Data are represented as the mean ± SEM of relative values of expression in 4 individual experiments (*$P < .05$). (*B*) Western blot analysis for Cox-2 in the colon. Immunoblots of tissue lysate proteins (25 μg/lane) prepared from colonic samples of TLR4−/− and MyD88−/−, and WT control mice before and after 7 days of DSS treatment. Membranes were probed with Cox-2 antibody. Positive control consists of cell lysate from LPS (2 μg/mL)-stimulated RAW264.7 cells (*right lane*). Cox-2 protein expression was greater in WT colon. Data are 1 representative experiment of 3 independent studies. β-actin was used as an internal control for protein loading. (*C*) Immunofluorescent staining for Cox-2 in the colon before and after 7 days of DSS treatment. Before DSS treatment, colonic tissue does not express detectable levels of Cox-2 in either (*C*) TLR4−/− mice or (*A*) WT controls. Immunofluorescent signal (*red* color of rhodamine) of Cox-2 was strongly detected in the colonic epithelial cytoplasm (*arrow*) and lamina propria cells (*arrowhead*) in (*B*) WT mice, but is very low in (*D*) TLR4−/− mice after DSS treatment. *Insets* show phase-contrast images identifying the orientation of colonic sections. (*D*) Expression of Cox-2 by lamina propria macrophages using double-staining of Cox-2 (fluorescein isothiocyanate green) and CD68 (TRITC *red*). Most Cox-2–positive lamina propria cells were double-stained with CD68 (macrophage marker). Representative data are from WT mice treated with 7 days of DSS. *Arrows* indicate double-positive cells showing *yellow* cytoplasmic staining. TLR4−/− mice do not have Cox-2–positive lamina propria macrophages (see *C*). (*E*) PGE_2 production in DSS-induced colitis. Colonic tissues from TLR4−/− and WT controls before and after 7 days of DSS were cultured in media for 24 hours and the concentration of PGE_2 in the supernatants was analyzed by EIA (n = 4 for each group). Data are represented as the mean ± SD of duplicate samples taken from 3 individual experiments. There was a significant difference in PGE_2 production in TLR4−/− mice after DSS treatment compared with WT mice (*$P < .05$).

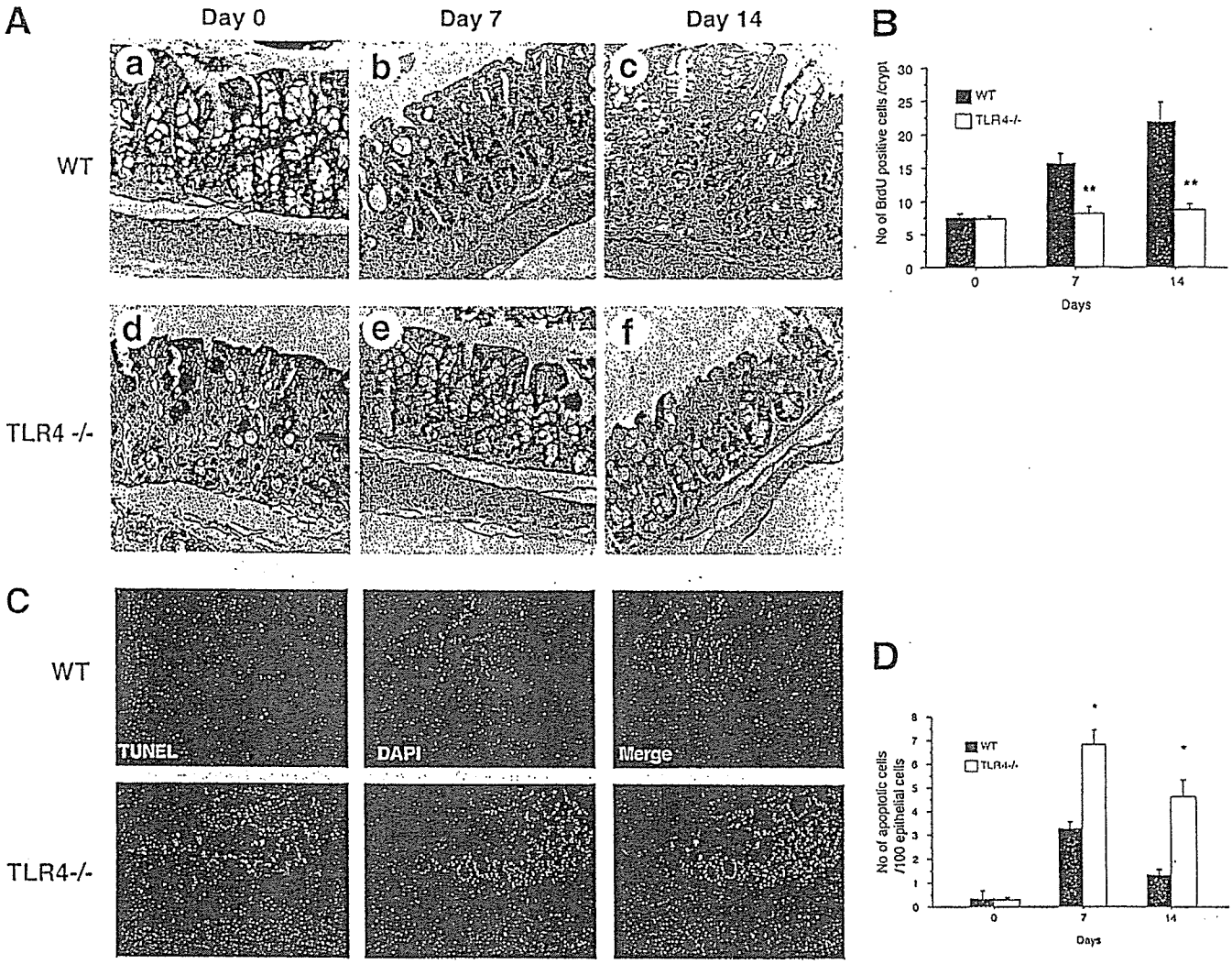

Figure 3. TLR4−/− mice have a persistent decrease in epithelial proliferation and increased apoptosis after 7 days of DSS treatment. (*A*) TLR4−/− and WT control mice were treated with 2.5% DSS for 7 days (*left panels*) followed by 7 days of recovery (*right panels*). Animals were injected with BrdU 90 minutes before death. Colonic sections taken from day 0 (*a*, WT; *d*, TLR4−/−), day 7 (*b*, WT; *e*, TLR4−/−), and day 14 (*c*, WT; *f*, TLR4−/−) were stained with anti-BrdU. BrdU-positive cells are identified by *black* staining of nuclei. TLR4−/− mice have fewer BrdU-positive cells in the crypts on (*e*) day 7 and on (*f*) day 14. Tissues were counterstained with methyl *green* (original magnification, 200×). (*B*) BrdU-positive cells were counted in 3 crypts of each colon segment per high-power field (9 crypts/mouse). *Bars* show the mean ± SEM of proliferating cells/crypts (n = 3 for each group on day 0 [ie, untreated], n = 5 for the other groups). The proliferating cells in TLR4−/− mice were significantly fewer than in WT controls after 7 days of DSS treatment (day 7) and during recovery (day 14) from DSS-induced colitis (***P* < .001). (*C*) Apoptotic cells in the colonic crypt epithelial cells of TLR4−/− and WT controls were determined by TUNEL assay. Representative sections were taken on day 7 of DSS treatment. *Red* staining of nuclei indicates apoptotic cells, which was observed mainly in the surface epithelium. Sections were counterstained with 4′,6-diamidino-2-phenylindole (*blue*) to identify the orientation of nuclei. TLR4−/− mice showed increased apoptotic cells compared with WT controls (original magnification, 200×). (*D*) Numbers of apoptotic cells were counted in 300 total epithelial cells in 3 areas of each colon segment (n = 3 for each group on day 0 [untreated], n = 6–7 for the other groups). *Bars* show the mean ± SEM of the number of apoptotic cells per 100 total nuclei of the epithelial cells. There were significant increases of apoptotic cells in TLR4−/− mice compared with WT controls after 7 days of DSS treatment (**P* < .05). The apoptotic cells were still increased in TLR4−/− mice even after recovery (day 14, **P* < .05).

namely worse clinical signs of colitis and abnormal proliferation and apoptosis. To test this hypothesis, TLR4−/− mice were given PGE_2 by oral gavage twice a day concurrently with the DSS treatment period. These mice were compared with TLR4−/− mice and WT mice given DSS alone with PBS to control for the gavage solution. Compared with TLR4−/− PBS-treated mice, TLR4−/− mice treated with PGE_2 behaved similar to WT mice with respect to weight loss (Figure 4*A*) and rectal bleeding (Figure 4*B*). We next examined the effect of PGE_2 supplementation on proliferation and apoptosis. TLR4−/− mice given PGE_2 had significantly greater proliferation (Figure 4*C* and *D*) and reduced apoptosis (Figure 4*E* and *F*) than TLR4−/− mice given vehicle alone. Total histology scores were lower for PGE_2-treated TLR4−/− mice compared with control TLR4−/− mice because crypt damage was less (data not shown). PGE_2 treatment of wild-type DSS-treated mice showed no significant change in proliferation (WT cont, 14.5 ± 1.4; WT + PGE_2, 12.3 ± 1.6) and a small decrease in apoptosis (WT

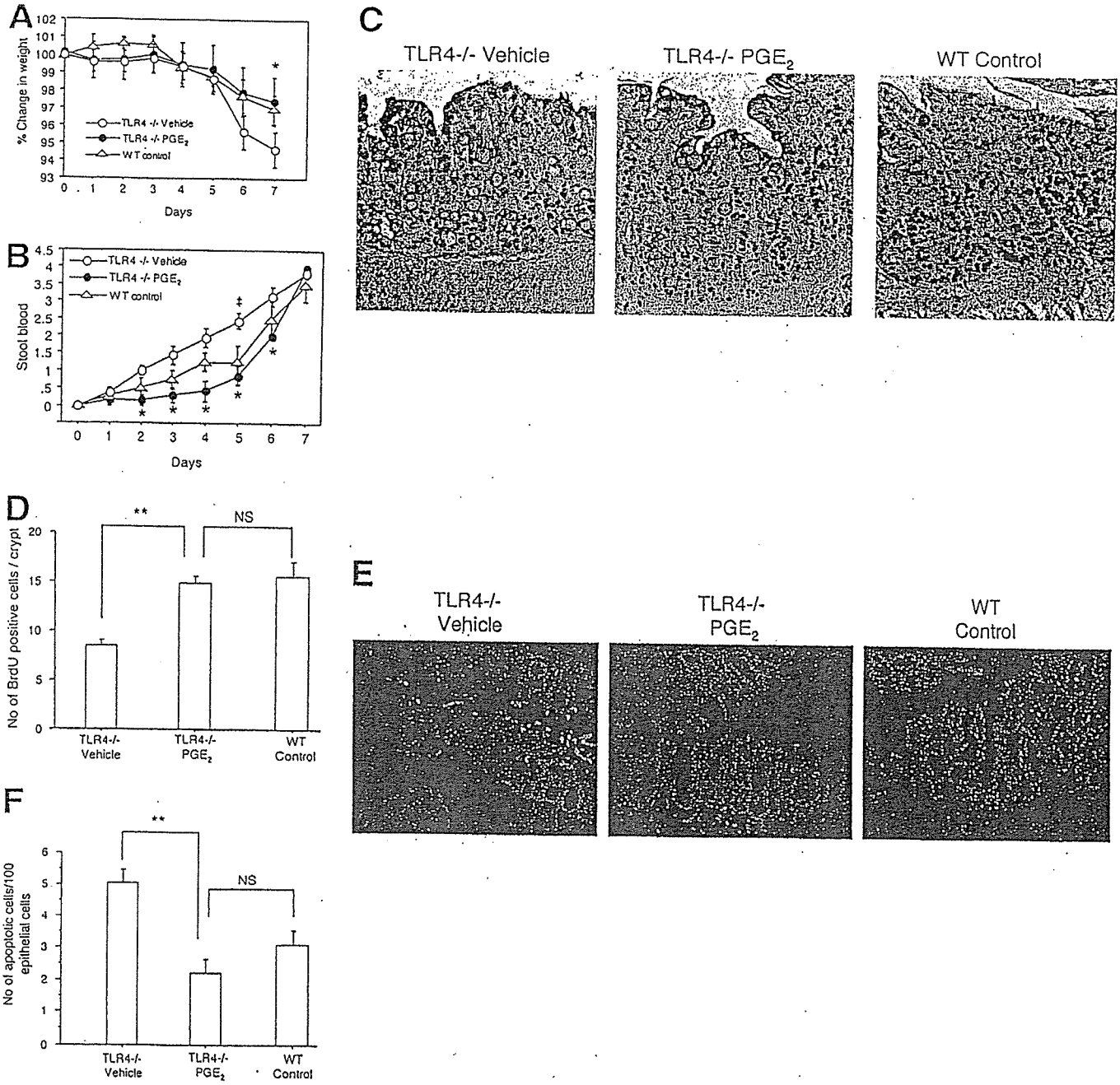

Figure 4. PGE_2 supplementation improves signs of colitis and restores epithelial healing after DSS-induced injury in TLR4−/− mice. (*A*) Weight change was examined daily during the 7 days of DSS treatment. Vehicle-treated (PBS) TLR4−/− mice had significantly more weight loss than WT control mice (*$P < .05$). PGE_2-treated TLR4−/− mice had significantly less weight loss than vehicle-treated TLR4−/− mice and are comparable with WT mice. The data represent the average (±SEM) of 3 independent experiments with a total of 19 mice (TLR4−/− vehicle [n = 6], TLR4−/− PGE_2 [n = 7], and WT controls [n = 6]). (*B*) PGE_2-treated TLR4−/− mice had a significant reduction in bleeding on days 2–6 compared with vehicle-treated (PBS) TLR4−/− mice (*$P < .05$). Stool blood was calculated as follows: 0 = no blood, 1 = trace occult blood positive, 2 = strongly occult blood positive, and 4 = bloody diarrhea. Standard error is shown. (*C*) BrdU labeling of intestinal epithelial cells was performed for vehicle-treated TLR4 −/−, PGE_2-treated TLR4−/−, and WT controls at the end of 7 days of DSS treatment (original magnification, 200×). (*D*) BrdU-positive cells were counted per high-power field in 3 crypts of each colon segment (9 areas/mouse). *Bars* show the mean ± SEM of proliferating cells/crypts (n = 5 in each group). There is a significant increase in BrdU-positive cells in PGE_2-treated TLR4−/− mice compared with vehicle-treated TLR4−/− mice (**$P < .001$). PGE_2-treated TLR4−/− mice are not significantly different than WT mice. (*E*) Apoptotic cells in the crypt epithelial cells were determined by TUNEL assay. Representative sections were taken from vehicle-treated TLR4−/−, PGE_2-treated TLR4−/− mice, and WT controls as indicated. *Red* staining of nuclei indicates apoptotic cells. Sections were counterstained with 4′,6-diamidino-2-phenylindole (*blue*) to identify the nuclei of epithelial cells. PGE_2-treated TLR4−/− mice showed a marked decrease of apoptotic cells compared with vehicle-treated TLR−/− mice. The frequency of TUNEL-positive epithelial cells in PGE_2-treated TLR4−/− mice was similar to WT controls (original magnification, 200×). (*F*) Number of apoptotic cells was counted in 300 total epithelial cells in triplicate in 3 areas for each colon segment (n = 5 in each group). *Bars* show the mean ± SEM of the number of apoptotic cells per 100 total nuclei in the epithelial cells counted. There is a significant decrease of apoptotic cells in PGE_2-treated TLR4−/− mice compared with vehicle-treated TLR4−/− mice (**$P < .001$).

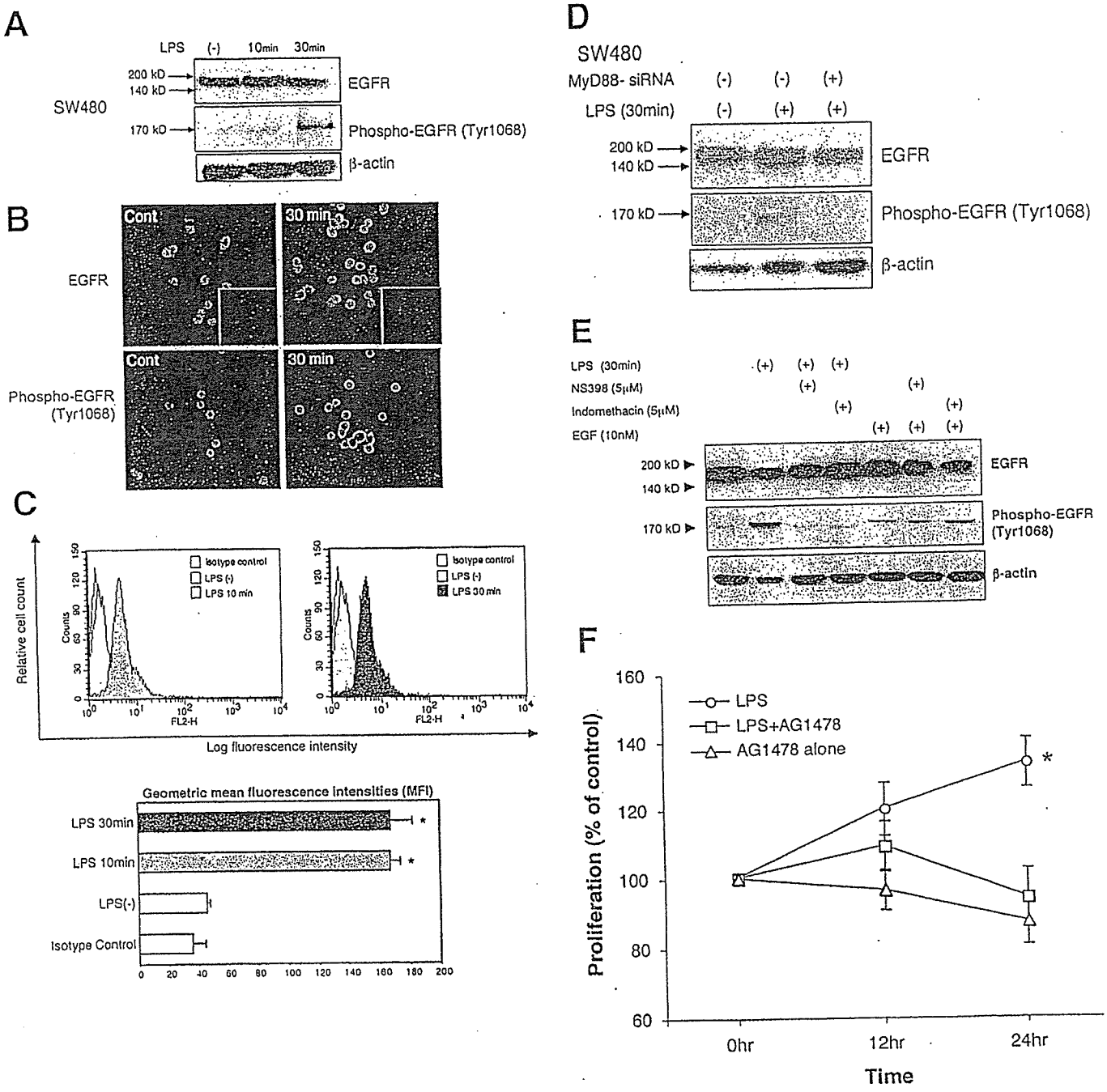

Figure 5. LPS induces EGFR phosphorylation in a MyD88-dependent fashion. (*A*) Western blot analysis of EGFR and its phosphorylation in human intestinal epithelial cell line SW480. Cells were stimulated with LPS for indicated periods. Blots of whole-cell lysates (25 μg/*lane*) were probed with either EGFR (*top panel*) or phosphorylated EGFR (*bottom panel*). LPS stimulated EGFR phosphorylation. Data are 1 representative experiment of 3 independent experiments with similar results. (*B*) Immunofluorescent staining for EGFR and phospho-EGFR in SW480. Cells were cultured on glass slides and treated with LPS (2 μg/mL) for indicated periods. Nuclei were stained with 4',6-diamidino-2-phenylindole. After 30 minutes of stimulation, confocal images show an increased intensity of staining of phospho-EGFR but not EGFR. *Insets* show negative control in which primary antibodies were omitted. Original magnification, 400×. (*C*) Flow cytometric analysis of phospho-EGFR (Tyr1068) after stimulation with LPS for indicated periods of time. Histograms show an increase in log fluorescence intensity. *Bars* represent the geometric mean of fluorescence intensity of phospho-EGFR-positive cells ± SD based on 3 individual experiments (LPS, 2 μg/mL) with triplicate samples (*$P < .05$). (*D*) LPS-induced EGFR phosphorylation is MyD88 dependent. Western blot analysis of EGFR and its phosphorylated form are shown. Cells were stimulated with LPS for indicated periods. Blots of whole-cell lysates (25 μg/*lane*) were probed with EGFR or phospho-EGFR antibody. Cells transfected with MyD88 siRNA had no phosphorylation of EGFR in response to LPS. Data are 1 representative experiment of 3 independent experiments with similar results. (*E*) LPS-induced EGFR phosphorylation is Cox-2 dependent. Cells were stimulated with LPS (2 μg/mL) for 30 minutes with or without Cox inhibitors as indicated, and whole-cell lysates (22 μg/*lane*) were probed with EGFR or phospho-EGFR antibodies. Western blot analysis shows that EGFR phosphorylation is inhibited by a nonselective Cox-2 inhibitor, (NS398 5 μmol/L), or a Cox-1 and Cox-2 inhibitor (indomethacin selective, 5 μmol/L). As a control, EGF (10 nMol = 6 ng/mL) was added to cells for 30 minutes. EGF-mediated phosphorylation of the EGFR was not inhibited by Cox inhibitors (last 3 *lanes*). Data are 1 representative experiment of 5 independent experiments with similar results. (*F*) LPS induced cell proliferation via EGFR activation. SW480 cells were stimulated with LPS (2 μg/mL) for indicated periods with or without EGFR-specific tyrosine kinase inhibitor AG1478. Data are shown as the means ± SD of percentage of absorbance in comparison with nontreated control cells from 3 independent experiments.

cont, 3.1 ± 2; WT + PGE_2, 1.4 ± 1.3). These data suggest that PGE_2 is necessary and sufficient to restore epithelial healing as measured by proliferation and apoptosis in the injured intestinal epithelium.

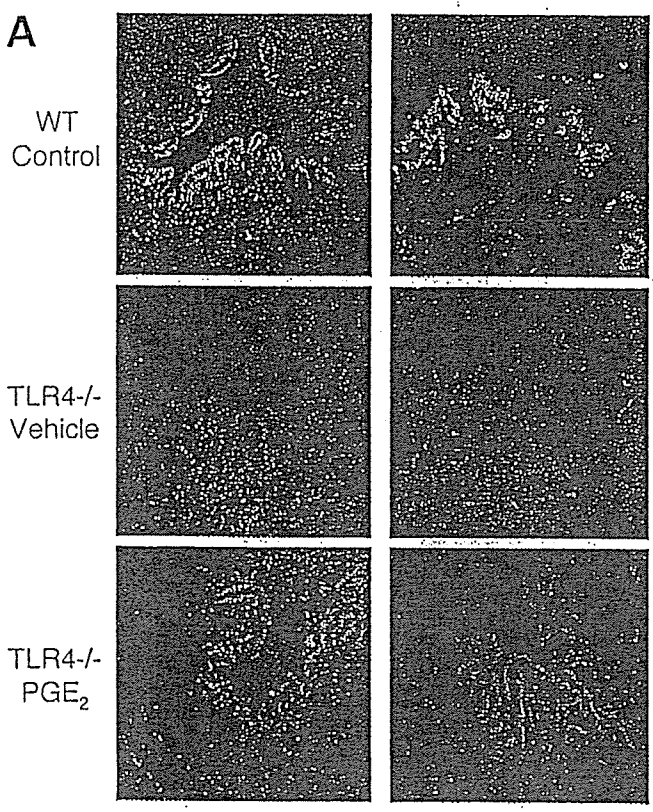

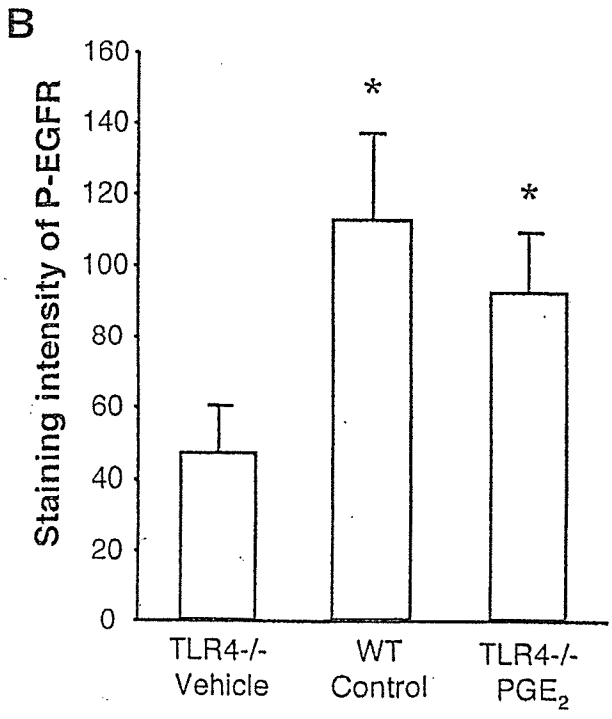

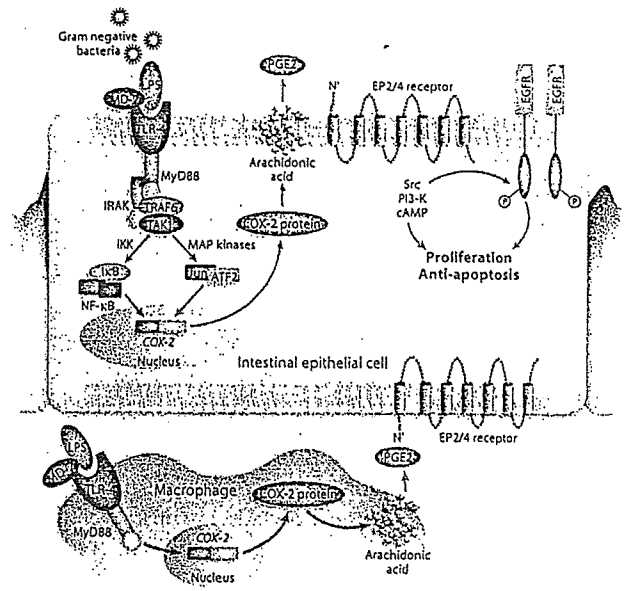

Figure 7. Model of TLR4-mediated Cox-2 regulation. In the setting of intestinal injury, LPS exposure of intestinal epithelial cells (possibly basolaterally) and lamina propria macrophages results in TLR4 activation and signaling via MyD88. This activates a variety of signaling pathways culminating in transcription factor translocation and engagement of the Cox-2 promoter. Cox-2 is transcribed and translated; it acts on arachidonic acid to generate PGG_2, which is converted rapidly to PGH_2 and then microsomal PGE synthase-1 converts it to PGE_2. PGE_2, through its receptors EP2 or EP4, can activate downstream signaling molecules such as the tyrosine kinase Src or the lipid kinase PI'3 kinase, which can lead to transactivation of EGFR. EGFR signaling is associated with proliferation and protection against apoptosis in intestinal epithelial cells. PGE_2 produced by macrophages also may act in *trans* on intestinal epithelial cells. In the absence of TLR4 signaling, Cox-2 expression is greatly decreased.

TLR4 Regulates Phosphorylation of the EGFR in Intestinal Epithelial Cells

Our data point to a link between TLR4-mediated induction of Cox-2 and PGE_2 production and intestinal injury. To understand the mechanism(s) by which PGE_2 mediates an effect on the intestinal epithelium, we examined the ability of LPS to stimulate EGFR phosphorylation. EGFR phosphorylation results in a variety of biologic events including induction of

Figure 6. TLR4−/− mice have decreased EGFR phosphorylation after DSS-induced colitis owing to defective production of mucosal PGE_2. (*A*) Immunofluorescent staining for phospho EGFR in the colon after 7 days of DSS treatment. Phosphorylated EGFR was strongly detected in surface epithelial cells in WT mice. PBS-treated TLR4−/− mice had decreased epithelial cell EGFR phosphorylation after DSS colitis. PGE_2 treatment partly restored the expression of phosphorylated EGFR. Two individual mouse tissue samples of each genotype with or without PGE_2 treatment are shown. (*B*) Quantification of the expression levels of phospho EGFR. Staining intensity of 10 randomly selected areas of epithelial cells per slide was analyzed using MetaMorph software. Staining intensity of phospho EGFR was decreased significantly in TLR4−/− mice compared with WT mice and PGE_2-treated TLR4−/− mice after 7 days of DSS treatment.

proliferation and protection against apoptosis.[43-46] PGE_2 mediates EGFR phosphorylation through induction of EGFR ligands or through intracellular mediators such as Src.[47,48] We hypothesized that LPS stimulation of intestinal epithelial cells would result in EGFR phosphorylation. SW480 cells were stimulated with LPS and total or phosphorylated EGFR was examined by Western blot and immunofluorescent staining (Figure *5A* and *B*). LPS stimulated phosphorylation of EGFR. We further quantified LPS-induced EGFR phosphorylation by flow cytometric analysis (Figure *5C*). LPS stimulation significantly increased EGFR phosphorylation. We then addressed whether this effect on EGFR was dependent on TLR–MyD88 signaling. EGFR phosphorylation was blocked by expression of MyD88 siRNA (Figure *5D*) and partially by a specific inhibitor of Cox-2, NS398 (Figure *5E*). EGF stimulation of SW480 cells resulted in EGFR phosphorylation that was not blocked by a Cox-2 inhibitor or indomethacin (Figure *5E*). Because it also was possible that LPS-induced EGFR phosphorylation is upstream of Cox-2 expression, we used a specific EGFR tyrosine kinase inhibitor, AG1478, and asked whether inhibition blocked LPS-mediated induction of Cox-2 protein expression. Inhibiting EGFR tyrosine kinase activity had no effect on Cox-2 induction (data not shown). Finally, we asked whether inhibition of EGFR phosphorylation affected LPS-induced cell proliferation in SW480 cells. AG1478 blocked LPS-induced cell proliferation (Figure *5F*). These data suggest that TLR4-mediated induction of PGE_2 production may stimulate epithelial proliferation by an EGFR-dependent mechanism.

Given the results of TLR4-regulating phosphorylation of EGFR in vitro, we hypothesized that TLR4−/− mice have decreased phosphorylation of EGFR in intestinal epithelial cells in vivo. To test this hypothesis, we used immunohistochemistry to evaluate the expression of phosphorylated EGFR in intestinal epithelial cells after DSS-induced colitis. WT mice had significantly higher expression of phosphorylated EGFR in intestinal epithelial cells than TLR4−/− mice after DSS-induced colitis (Figure *6A*). TLR4−/− mice given PGE_2 treatment had restored expression of phosphorylated EGFR to nearly WT levels (Figure *6A*). Omission of primary antibody did not show any staining (data not shown). Computer analysis using the MetaMorph program was used to quantify intensity of staining in the intestinal epithelium (Figure *6B*). We conclude from these results that impaired epithelial repair seen in TLR4−/− mice is at least partly owing to impaired activation of epithelial cell EGFR, which in turn may be owing to decreased mucosal production of PGE_2 in response to inflammation.

Discussion

In this study, we show a requirement for TLR4 in regulating Cox-2 expression in both intestinal epithelial cells and lamina propria macrophages. In our model (Figure 7), epithelial injury permits exposure of intestinal epithelial cells and lamina propria macrophages to gram-negative bacteria and LPS. TLR4 signaling via MyD88 activates a signaling cascade that results in enhanced transcription of *Cox-2* and increased production of PGE_2. The clinical manifestations of increased rectal bleeding seen in TLR4[3] mice likely are caused by the epithelial defect in proliferation and apoptosis because correcting the defect with native exogenous PGE_2 restored mice to WT levels of rectal bleeding. These data suggest that a relative deficiency in PGE_2 production is likely to play an important role in the observed TLR4[3] phenotype. Our in vitro data support the idea that the effect of TLR4 on Cox-2 expression and other downstream mediators of epithelial repair can occur directly by LPS signaling in intestinal epithelial cells. In vivo, however, there is likely to be a contribution by lamina propria macrophages acting in *trans* on the epithelium by way of contact or secreted factors including PGE_2.

We present data that the colonic epithelium depends on bacterial-derived signals to activate the complex program involved in tissue repair. With the discovery of TLR molecules, the exact pathways by which this occurs may be better understood. The notion that TLR signaling is relevant and necessary for repair of injury is exemplified in a recent study showing that mice deficient in MyD88 or TLR4/TLR2 signaling were impaired in their ability to heal after acute lung injury.[49] The authors describe that extracellular matrix hyaluronan, either directly or indirectly, activates TLR2 and TLR4 signaling, resulting in inflammatory cell transmigration and protection against apoptosis. In the absence of TLR signaling there is decreased inflammatory infiltrate in the lungs of mice, but paradoxically animals have decreased survival. The similarities of our results in a model of intestinal epithelial cell injury suggest a common theme of repair linked to an inflammatory signal.

To understand what role TLR4 might be playing in the setting of DSS-induced injury we examined the literature for known effects of LPS on the intestinal epithelium. Investigators have shown that LPS can induce proliferation of intestinal epithelial cell (IEC)-6 cells in culture through a tumor necrosis factor–dependent mechanism.[50] Grishin et al[51,52] recently showed that LPS stimulates Cox-2 in a rat intestinal epithelial cell line and have focused on the role this may play in necrotizing enterocolitis. Although our study is not the first to show a link between LPS and Cox-2, we believe our studies show the degree to which TLR4 is required for intestinal expression of Cox-2 in vivo and the dependence of TLR4-mediated Cox-2 expression in repair of the damaged epithelium. Rakoff-Nahoum et al[14] examined proliferation in MyD88−/− mice in the setting of radiation injury and found a decrease in proliferative response but did not investigate the underlying mechanism in detail. Finally, Pull et al[3] used a bone-marrow chimera model to look at the relative contribution of MyD88 expression in immune vs nonimmune cells in the colonic proliferative response after DSS colitis. They describe a prominent role for MyD88-expressing lamina propria mesenchymal cells in the proliferative response of the epithelium in DSS-treated mice. Interestingly, in supplemental material accompanying the article by Pull et al,[3] Cox-2 was expressed highly in mesenchyme derived from conventionalized RAG1−/− mouse intestine compared with MyD88−/− mice, suggesting that the Cox-2 from mesenchymal cells may play a role in epithelial repair. Given the broad nature of the defect in TLR, interleukin-1, and interleukin-18 signaling in MyD88−/− cells, the prior studies do not address the specific contribution of TLR4 signaling nor the mechanisms underlying the proliferative defect.

Other studies were performed before the identification of TLR4 as the receptor for LPS. Studies in C3H/HeJ mice with a mutation in TLR4[8] found that crypt epithelial proliferation was decreased after DSS and could be restored by PGE_2.[53] Similar to Wang et al,[54] we used native PGE_2 administered orally rather than the longer-acting dimethyl-PGE_2. We used oral PGE_2 be-

cause of previous evidence that this approach led to increased levels of PGE_2 in the blood and intestine and altered colon physiology. Riehl et al[21] described that systemic LPS protected against radiation-induced epithelial apoptosis in intestinal crypts through a mechanism that depends on PGE_2 production.

The link between Cox-2 and PGE_2 in protection from colitis is highlighted in a variety of studies. Cox-2−/− mice show increased susceptibility to DSS-induced colitis, which correlates with their inability to produce PGE_2.[22] Animals deficient in the PGE_2 receptor, EP4, are more susceptible to DSS injury.[55] Several mechanisms underlie the protective effects of PGE_2. PGE_2, through its receptors EP2 or EP4, may stimulate EGFR phosphorylation through intracellular kinases such as Src or by increased expression of amphiregulin, an EGFR ligand.[46-48,56] PGE_2 protects against radiation-induced intestinal epithelial cell apoptosis through an EGFR and Akt-dependent effect on Bax.[48] Signaling downstream of EGFR is involved in growth, repair, and barrier integrity of the gastrointestinal mucosa.[57-59] Increased susceptibility of EGFR-deficient mice to DSS-induced colitis also has been reported.[60]

Studies also have shown that Cox-2 levels[41] and PGE_2 production[61-63] are increased in inflammatory bowel disease. Cox-2 overexpression characterizes dysplasia and colon cancer.[64-66] Recent work shows that PGE_2-dependent colon carcinogenesis involves deregulated phosphoinositide 3 (PI-3) kinase signaling and increased expression of β-catenin.[67] An increase in EGFR phosphorylation has been described in the mucosa of patients with ulcerative colitis.[68] This model is consistent with the known benefit of Cox-2 inhibitors and EGFR antagonists such as cetuximab in the prevention or treatment of colon cancer. In IBD, it remains controversial whether Cox-2 inhibitors worsen symptoms of the disease.[69] Short-term studies have shown that Cox-2 inhibitors do not flare colitis,[70] but long-term use, as would be required for chemoprevention, might flare disease. Mesalamines inhibit arachidonic acid metabolism to PGE_2 and have a modest chemopreventive benefit in patients with ulcerative colitis,[71] whereas other immunomodulators such as 6-mercaptopurine do not.[72] These data suggest an inflammation-independent effect of mesalamines, possibly through inhibition of PGE_2.

Our studies highlight the previous unknown dependence of Cox-2 expression by TLR4 in the intestine. In the acute response to injury, TLR4 signaling results in increased Cox-2 and PGE_2 production, which is beneficial. We may speculate that long-term, persistent TLR4 signaling may contribute to colitis-associated cancers. Strategies aimed at dampening TLR4 signaling may reduce chronic inflammation and the drive toward carcinogenesis.

References

1. Hooper LV, Stappenbeck TS, Hong CV, Gordon JI. Angiogenins: a new class of microbicidal proteins involved in innate immunity. Nat Immunol 2003;4:269–273.
2. Abrams GD, Bauer H, Sprinz H. Influence of the normal flora on mucosal morphology and cellular renewal in the ileum. A comparison of germ-free and conventional mice. Lab Invest 1963;12:355–364.
3. Pull SL, Doherty JM, Mills JC, Gordon JI, Stappenbeck TS. Activated macrophages are an adaptive element of the colonic epithelial progenitor niche necessary for regenerative responses to injury. Proc Natl Acad Sci U S A 2005;102:99–104.
4. Kitajima S, Morimoto M, Sagara E, Shimizu C, Ikeda Y. Dextran sodium sulfate-induced colitis in germ-free IQI/Jic mice. Exp Anim 2001;50:387–395.
5. Sartor RB. Clinical applications of advances in the genetics of IBD. Rev Gastroenterol Disord 2003;3:S9–S17.
6. Kim SC, Tonkonogy SL, Albright CA, Tsang J, Balish EJ, Braun J, Huycke MM, Sartor RB. Variable phenotypes of enterocolitis in interleukin 10-deficient mice monoassociated with two different commensal bacteria. Gastroenterology 2005;128:891–906.
7. Pasare C, Medzhitov R. Toll-like receptors: linking innate and adaptive immunity. Adv Exp Med Biol 2005;560:11–18.
8. Poltorak A, He X, Smirnova I, Liu MY, Huffel CV, Du X, Birdwell D, Alejos E, Silva M, Galanos C, Freudenberg M, Ricciardi-Castagnoli P, Layton B, Beutler B. Defective LPS signaling in C3H/HeJ and C57BL/10ScCr mice: mutations in Tlr4 gene. Science 1998;282:2085–2088.
9. Hoshino K, Takeuchi O, Kawai T, Sanjo H, Ogawa T, Takeda Y, Takeda K, Akira S. Cutting edge: Toll-like receptor 4 (TLR4)-deficient mice are hyporesponsive to lipopolysaccharide: evidence for TLR4 as the Lps gene product. J Immunol 1999;162:3749–3752.
10. Travassos LH, Girardin SE, Philpott DJ, Blanot D, Nahori MA, Werts C, Boneca IG. Toll-like receptor 2-dependent bacterial sensing does not occur via peptidoglycan recognition. EMBO Rep 2004;5:1000–1006.
11. Sato S, Sanjo H, Takeda K, Ninomiya-Tsuji J, Yamamoto M, Kawai T, Matsumoto K, Takeuchi O, Akira S. Essential function for the kinase TAK1 in innate and adaptive immune responses. Nat Immunol 2005;6:1087–1095.
12. Cario E, Gerken G, Podolsky DK. Toll-like receptor 2 enhances ZO-1-associated intestinal epithelial barrier integrity via protein kinase C. Gastroenterology 2004;127:224–238.
13. Vora P, Youdim A, Thomas LS, Fukata M, Tesfay SY, Lukasek K, Michelsen KS, Wada A, Hirayama T, Arditi M, Abreu MT. Beta-defensin-2 expression is regulated by TLR signaling in intestinal epithelial cells. J Immunol 2004;173:5398–5405.
14. Rakoff-Nahoum S, Paglino J, Eslami-Varzaneh F, Edberg S, Medzhitov R. Recognition of commensal microflora by Toll-like receptors is required for intestinal homeostasis. Cell 2004;118:229–241.
15. Fukata M, Michelsen KS, Eri R, Thomas LS, Hu B, Lukasek K, Nast CC, Lechago J, Xu R, Naiki Y, Soliman A, Arditi M, Abreu MT. Toll-like receptor-4 is required for intestinal response to epithelial injury and limiting bacterial translocation in a murine model of acute colitis. Am J Physiol 2005;288:G1055–G1065.
16. Araki A, Kanai T, Ishikura T, Makita S, Uraushihara K, Iiyama R, Totsuka T, Takeda K, Akira S, Watanabe M. MyD88-deficient mice develop severe intestinal inflammation in dextran sodium sulfate colitis. J Gastroenterol 2005;40:16–23.
17. Backlund MG, Mann JR, Holla VR, Buchanan FG, Tai HH, Musiek ES, Milne GL, Katkuri S, DuBois RN. 15-Hydroxyprostaglandin dehydrogenase is down-regulated in colorectal cancer. J Biol Chem 2005;280:3217–3223.
18. Subbaramaiah K, Yoshimatsu K, Scherl E, Das KM, Glazier KD, Golijanin D, Soslow RA, Tanabe T, Naraba H, Dannenberg AJ. Microsomal prostaglandin E synthase-1 is overexpressed in inflammatory bowel disease. Evidence for involvement of the transcription factor Egr-1. J Biol Chem 2004;279:12647–12658.
19. Otani T, Yamaguchi K, Scherl E, Du B, Tai HH, Greifer M, Petrovic L, Daikoku T, Dey SK, Subbaramaiah K, Dannenberg AJ. Levels of NAD(+)-dependent 15-hydroxyprostaglandin dehydrogenase are reduced in inflammatory bowel disease: evidence for involvement of TNF-alpha. Am J Physiol 2006;290:G361–G368.
20. Newberry RD, McDonough JS, Stenson WF, Lorenz RG. Spontaneous and continuous cyclooxygenase-2-dependent prostaglandin E2 production by stromal cells in the murine small intestine

lamina propria: directing the tone of the intestinal immune response. J Immunol 2001;166:4465–4472.
21. Riehl T, Cohn S, Tessner T, Schloemann S, Stenson WF. Lipopolysaccharide is radioprotective in the mouse intestine through a prostaglandin-mediated mechanism. Gastroenterology 2000; 118:1106–1116.
22. Morteau O, Morham SG, Sellon R, Dieleman LA, Langenbach R, Smithies O, Sartor RB. Impaired mucosal defense to acute colonic injury in mice lacking cyclooxygenase-1 or cyclooxygenase-2. J Clin Invest 2000;105:469–478.
23. Wang D, Buchanan FG, Wang H, Dey SK, DuBois RN. Prostaglandin E2 enhances intestinal adenoma growth via activation of the Ras-mitogen-activated protein kinase cascade. Cancer Res 2005;65:1822–1829.
24. Holla VR, Wang D, Brown JR, Mann JR, Katkuri S, DuBois RN. Prostaglandin E2 regulates the complement inhibitor CD55/decay-accelerating factor in colorectal cancer. J Biol Chem 2005; 280:476–483.
25. Atreya R, Mudter J, Finotto S, Mullberg J, Jostock T, Wirtz S, Schutz M, Bartsch B, Holtmann M, Becker C, Strand D, Czaja J, Schlaak JF, Lehr HA, Autschbach F, Schurmann G, Nishimoto N, Yoshizaki K, Ito H, Kishimoto T, Galle PR, Rose-John S, Neurath MF. Blockade of interleukin 6 trans signaling suppresses T-cell resistance against apoptosis in chronic intestinal inflammation: evidence in Crohn disease and experimental colitis in vivo. Nat Med 2000;6:583–588.
26. Cooper HS, Murthy SN, Shah RS, Sedergran DJ. Clinicopathologic study of dextran sulfate sodium experimental murine colitis. Lab Invest 1993;69:238–249.
27. Siegmund B, Lehr HA, Fantuzzi G. Leptin: a pivotal mediator of intestinal inflammation in mice. Gastroenterology 2002;122:2011–2025.
28. Moss SF, Holt PR. Apoptosis in the intestine. Gastroenterology 1996;111:567–568.
29. Inoue H, Nanayama T, Hara S, Yokoyama C, Tanabe T. The cyclic AMP response element plays an essential role in the expression of the human prostaglandin-endoperoxide synthase 2 gene in differentiated U937 monocytic cells. FEBS Lett 1994;350:51–54.
30. Inoue H, Yokoyama C, Hara S, Tone Y, Tanabe T. Transcriptional regulation of human prostaglandin-endoperoxide synthase-2 gene by lipopolysaccharide and phorbol ester in vascular endothelial cells. Involvement of both nuclear factor for interleukin-6 expression site and cAMP response element. J Biol Chem 1995; 270:24965–24971.
31. Mukherji M. Phosphoproteomics in analyzing signaling pathways. Expert Rev Proteomics 2005;2:117–128.
32. Irish JM, Hovland R, Krutzik PO, Perez OD, Bruserud O, Gjertsen BT, Nolan GP. Single cell profiling of potentiated phospho-protein networks in cancer cells. Cell 2004;118:217–228.
33. Rhee SH, Hwang D. Murine Toll-like receptor 4 confers lipopolysaccharide responsiveness as determined by activation of NF kappa B and expression of the inducible cyclooxygenase. J Biol Chem 2000;275:34035–34040.
34. Suzuki M, Hisamatsu T, Podolsky DK. Gamma interferon augments the intracellular pathway for lipopolysaccharide (LPS) recognition in human intestinal epithelial cells through coordinated up-regulation of LPS uptake and expression of the intracellular Toll-like receptor 4-MD-2 complex. Infect Immun 2003;71:3503–3511.
35. Yoshimatsu K, Golijanin D, Paty PB, Soslow RA, Jakobsson PJ, DeLellis RA, Subbaramaiah K, Dannenberg AJ. Inducible microsomal prostaglandin E synthase is overexpressed in colorectal adenomas and cancer. Clin Cancer Res 2001;7:3971–3976.
36. Backlund MG, Mann JR, Dubois RN. Mechanisms for the prevention of gastrointestinal cancer: the role of prostaglandin E2. Oncology 2005;69(Suppl 1):28–32.
37. Meyer TA, Noguchi Y, Ogle CK, Tiao G, Wang JJ, Fischer JE, Hasselgren PO. Endotoxin stimulates interleukin-6 production in intestinal epithelial cells. A synergistic effect with prostaglandin E2. Arch Surg 1994;129:1290–1295.
38. Longo WE, Damore LJ, Mazuski JE, Smith GS, Panesar N, Kaminski DL. The role of cyclooxygenase-1 and cyclooxygenase-2 in lipopolysaccharide and interleukin-1 stimulated enterocyte prostanoid formation. Mediators Inflamm 1998;7:85–91.
39. Grossman EM, Longo WE, Mazuski JE, Panesar N, Kaminski DL. Role of cytoplasmic and secretory phospholipase A2 in intestinal epithelial cell prostaglandin E2 formation. Int J Surg Investig 2000;1:467–476.
40. Newberry RD, McDonough JS, Stenson WF, Lorenz RG. Spontaneous and continuous cyclooxygenase-2-dependent prostaglandin E2 production by stromal cells in the murine small intestine lamina propria: directing the tone of the intestinal immune response. J Immunol 2001;166:4465–4472.
41. Singer II, Kawka DW, Schloemann S, Tessner T, Riehl T, Stenson WF. Cyclooxygenase 2 is induced in colonic epithelial cells in inflammatory bowel disease. Gastroenterology 1998;115:297–306.
42. Watson AJ, Chu S, Sieck L, Gerasimenko O, Bullen T, Campbell F, McKenna M, Rose T, Montrose MH. Epithelial barrier function in vivo is sustained despite gaps in epithelial layers. Gastroenterology 2005;129:902–912.
43. Stern LE, Erwin CR, O'Brien DP, Huang F, Warner BW. Epidermal growth factor is critical for intestinal adaptation following small bowel resection. Microsc Res Tech 2000;51:138–148.
44. Podolsky DK. Mechanisms of regulatory peptide action in the gastrointestinal tract: trefoil peptides. J Gastroenterol 2000; 35(Suppl 12):69–74.
45. Wu R, Abramson AL, Shikowitz MJ, Dannenberg AJ, Steinberg BM. Epidermal growth factor-induced cyclooxygenase-2 expression is mediated through phosphatidylinositol-3 kinase, not mitogen-activated protein/extracellular signal-regulated kinase kinase, in recurrent respiratory papillomas. Clin Cancer Res 2005; 11:6155–6161.
46. Dannenberg AJ, Lippman SM, Mann JR, Subbaramaiah K, DuBois RN. Cyclooxygenase-2 and epidermal growth factor receptor: pharmacologic targets for chemoprevention. J Clin Oncol 2005; 23:254–266.
47. Pai R, Soreghan B, Szabo IL, Pavelka M, Baatar D, Tarnawski AS. Prostaglandin E2 transactivates EGF receptor: a novel mechanism for promoting colon cancer growth and gastrointestinal hypertrophy. Nat Med 2002;8:289–293.
48. Tessner TG, Muhale F, Riehl TE, Anant S, Stenson WF. Prostaglandin E2 reduces radiation-induced epithelial apoptosis through a mechanism involving AKT activation and bax translocation. J Clin Invest 2004;114:1676–1685.
49. Jiang D, Liang J, Fan J, Yu S, Chen S, Luo Y, Prestwich GD, Mascarenhas MM, Garg HG, Quinn DA, Homer RJ, Goldstein DR, Bucala R, Lee PJ, Medzhitov R, Noble PW. Regulation of lung injury and repair by Toll-like receptors and hyaluronan. Nat Med 2005;11:1173–1179.
50. Ruemmele FM, Beaulieu JF, Dionne S, Levy E, Seidman EG, Cerf-Bensussan N, Lentze MJ. Lipopolysaccharide modulation of normal enterocyte turnover by Toll-like receptors is mediated by endogenously produced tumour necrosis factor alpha. Gut 2002; 51:842–848.
51. Grishin AV, Wang J, Hackam DJ, Qureshi F, Upperman JS, Zamora R, Ford HR. p38 MAP kinase mediates endotoxin-induced expression of cyclooxygenase-2 in enterocytes. Surgery 2004;136: 329–335.
52. Grishin AV, Wang J, Potoka DA, Hackam DJ, Upperman JS, Boyle P, Zamora R, Ford HR. Lipopolysaccharide induces cyclooxygenase-2 in intestinal epithelium via a noncanonical p38 MAPK pathway. J Immunol 2006;176:580–588.

53. Tessner TG, Cohn SM, Schloemann S, Stenson WF. Prostaglandins prevent decreased epithelial cell proliferation associated with dextran sodium sulfate injury in mice. Gastroenterology 1998;115:874–882.
54. Wang D, Wang H, Shi Q, Katkuri S, Walhi W, Desvergne B, Das SK, Dey SK, DuBois RN. Prostaglandin E(2) promotes colorectal adenoma growth via transactivation of the nuclear peroxisome proliferator-activated receptor delta. Cancer Cell 2004;6:285–295.
55. Kabashima K, Saji T, Murata T, Nagamachi M, Matsuoka T, Segi E, Tsuboi K, Sugimoto Y, Kobayashi T, Miyachi Y, Ichikawa A, Narumiya S. The prostaglandin receptor EP4 suppresses colitis, mucosal damage and CD4 cell activation in the gut. J Clin Invest 2002;109:883–893.
56. Buchanan FG, Wang D, Bargiacchi F, DuBois RN. Prostaglandin E2 regulates cell migration via the intracellular activation of the epidermal growth factor receptor. J Biol Chem 2003;278:35451–35457.
57. Konturek PK, Brzozowski T, Konturek SJ, Dembinski A. Role of epidermal growth factor, prostaglandin, and sulfhydryls in stress-induced gastric lesions. Gastroenterology 1990;99:1607–1615.
58. Romano M, Polk WH, Awad JA, Arteaga CL, Nanney LB, Wargovich MJ, Kraus ER, Boland CR, Coffey RJ. Transforming growth factor alpha protection against drug-induced injury to the rat gastric mucosa in vivo. J Clin Invest 1992;90:2409–2421.
59. Playford RJ, Wright NA. Why is epidermal growth factor present in the gut lumen? Gut 1996;38:303–305.
60. Egger B, Buchler MW, Lakshmanan J, Moore P, Eysselein VE. Mice harboring a defective epidermal growth factor receptor (waved-2) have an increased susceptibility to acute dextran sulfate-induced colitis. Scand J Gastroenterol 2000;35:1181–1187.
61. Carty E, De Brabander M, Feakins RM, Rampton DS. Measurement of in vivo rectal mucosal cytokine and eicosanoid production in ulcerative colitis using filter paper. Gut 2000;46:487–492.
62. Sharon P, Ligumsky M, Rachmilewitz D, Zor U. Role of prostaglandins in ulcerative colitis. Enhanced production during active disease and inhibition by sulfasalazine. Gastroenterology 1978; 75:638–640.
63. Wiercinska-Drapalo A, Flisiak R, Prokopowicz D. Effects of ulcerative colitis activity on plasma and mucosal prostaglandin E2 concentration. Prostaglandins Other Lipid Mediat 1999;58:159–165.
64. Sheehan KM, O'Connell F, O'Grady A, Conroy RM, Leader MB, Byrne MF, Murray FE, Kay EW. The relationship between cyclooxygenase-2 expression and characteristics of malignant transformation in human colorectal adenomas. Eur J Gastroenterol Hepatol 2004;16:619–625.
65. Konturek PC, Kania J, Burnat G, Hahn EG, Konturek SJ. Prostaglandins as mediators of COX-2 derived carcinogenesis in gastrointestinal tract. J Physiol Pharmacol 2005;56(Suppl 5):57–73.
66. Wang D, Mann JR, DuBois RN. The role of prostaglandins and other eicosanoids in the gastrointestinal tract. Gastroenterology 2005;128:1445–1461.
67. Castellone MD, Teramoto H, Williams BO, Druey KM, Gutkind JS. Prostaglandin E2 promotes colon cancer cell growth through a Gs-axin-beta-catenin signaling axis. Science 2005;310:1504–1510.
68. Malecka-Panas E, Kordek R, Biernat W, Tureaud J, Liberski PP, Majumdar AP. Differential activation of total and EGF receptor (EGF-R) tyrosine kinase (tyr-k) in the rectal mucosa in patients with adenomatous polyps, ulcerative colitis and colon cancer. Hepatogastroenterology 1997;44:435–440.
69. Matuk R, Crawford J, Abreu MT, Targan SR, Vasiliauskas EA, Papadakis KA. The spectrum of gastrointestinal toxicity and effect on disease activity of selective cyclooxygenase-2 inhibitors in patients with inflammatory bowel disease. Inflamm Bowel Dis 2004;10:352–356.
70. Sandborn W, Stenson W, Brynskov J, Steidle G, Robbins J. Safety of celecoxib in patients with ulcerative colitis in remission: a randomized, double-blind, placebo-controlled study. Clin Gastroenterol Hepatol 2006;4:157–159.
71. Velayos FS, Terdiman JP, Walsh JM. Effect of 5-aminosalicylate use on colorectal cancer and dysplasia risk: a systematic review and metaanalysis of observational studies. Am J Gastroenterol 2005;100:1345–1353.
72. Matula S, Croog V, Itzkowitz S, Harpaz N, Bodian C, Hossain S, Ullman T. Chemoprevention of colorectal neoplasia in ulcerative colitis: the effect of 6-mercaptopurine. Clin Gastroenterol Hepatol 2005;3:1015–1021.

Received January 9, 2006. Accepted June 2, 2006.

Address requests for reprints to: Dr Maria T. Abreu, Division of Gastroenterology, Inflammatory Bowel Disease Center, Mt. Sinai School of Medicine, 1425 Madison Avenue, 11-23D, New York, New York 10029. e-mail: maria.abreau@mssm.edu; fax: (212) 659-9853.

Supported by National Institutes of Health grants AI052266 and DK069594 (M.T.A.), the New York Crohn's Foundation (A.J.D.), and a Uehara Memorial Foundation Research Fellowship (M.F.).

Dimerization Is Crucial for the Function of the Na^+/H^+ Exchanger NHE1†

Takashi Hisamitsu, Youssef Ben Ammar, Tomoe Y. Nakamura, and Shigeo Wakabayashi*

Department of Molecular Physiology, National Cardiovascular Center Research Institute, Suita, Osaka 565-8565, Japan

Received May 2, 2006; Revised Manuscript Received August 15, 2006

ABSTRACT: The Na^+/H^+ exchanger 1 (NHE1) exists as a homo-dimer in the plasma membranes. In the present study, we have investigated the functional significance of the dimerization, using two nonfunctional NHE1 mutants, surface-expression-deficient G309V and transport-deficient E262I. Biochemical and immunocytochemical experiments revealed that these NHE1 mutants are capable of interacting with the wild-type NHE1 and, thus, forming a heterodimer. Expression of G309V retained the wild-type NHE1 to the ER membranes, suggesting that NHE1 would first form a dimer in the ER. On the other hand, expression of E262I markedly reduced the exchange activity of the wild-type NHE1 through an acidic shift in the intracellular pH (pH_i) dependence, suggesting that dimerization is required for exchange activity in the physiological pH_i range. However, a dominant−negative effect of E262I was not detected when exchange activity was measured at acidic pH_i, implying that one active subunit is sufficient to catalyze ion transport when the intracellular H^+ concentration is sufficiently high. Furthermore, intermolecular cysteine cross-linking at extracellular position Ser^{375} with a bifunctional sulfhydryl reagent dramatically inhibited exchange activity mainly by inducing the acidic shift of pH_i dependence and abolished extracellular stimuli-induced activation of NHE1 without causing a large change in the affinities for extracellular Na^+ or an inhibitor EIPA. Because monofunctional sulfhydryl regents had no effect, it is likely that cross-linking inhibited the activity of NHE1 by restricting a coupled motion between the two subunits during transport. Taken together, these data support the view that dimerization of two active subunits are required for NHE1 to possess the exchange activity in the neutral pH_i range, although each subunit is capable of catalyzing transport in the acidic pH_i range.

The Na^+/H^+ exchanger (NHE[1]) is a member of the secondary active transporter family, which catalyzes the exchange of Na^+ for H^+ (*1*−*5*). NHE isoforms (NHE1−NHE9) possess a common structural feature, that is, the molecules have two large functional domains, an amino (*N*-) terminal membrane domain consisting of multiple membrane-spanning helices and a long carboxyl (*C*-) terminal hydrophilic domain. Of nine known isoforms, NHE1 is ubiquitously expressed and is responsible for the control of intracellular pH (pH_i) and cell volume (*1*−*5*). NHE1 is known to be activated in response to various extrinsic stimuli such as hormones, growth factors, and changes in the medium osmolarity, presumably through the interaction of various signaling molecules with the *C*-terminal cytoplasmic domain. Importantly, such activation of NHE1 is thought to be exerted through a conformational change of the exchanger molecule, which is triggered by protonation at a H^+-modifier or pH sensor site that is distinct from the H^+-transport site (*6*−*8*).

In contrast to the extensive studies investigating the regulatory mechanism of NHE1, structural information including the subunit-subunit interaction is extremely limited. A previous study showed that NHE1 and NHE3 form homo-oligomers by interacting via the transmembrane regions in intact cells (*9*), and consistent with this, NHE1 in the placental brush border membranes was detected as a larger form (~205 kDa), cross-linked by disulfide bonds (*10*). Furthermore, we recently presented evidence that NHE1 forms a homodimer but not a homotrimer or a homotetramer (*11*). Despite detailed descriptions of the oligomeric state of the exchanger, its functional significance is not well understood. The previous study (*9*) suggested that the functional unit of NHE1 is a monomer on the basis of the coexpression experiment of transport-deficient mutant E262I. However, it has been reported that the interaction between

† This work was supported by a Grant-in-Aid for Priority Areas 13142210 for Scientific Research from the Ministry of Education, Science Culture of Japan, by Grant nano-001 for Research on Advanced Medical Technology from the Ministry of Health, Labor, and Welfare of Japan, and by the Program for Promotion of Fundamental Studies in Health Science of the National Institute of Biomedical Innovation (NIBIO).

* To whom correspondence should be addressed. Tel: 81-6-6833-5012. Fax: 81-6-6835-5314. E-mail: wak@ri.ncvc.go.jp.

[1] Abbreviations: NHE, Na^+/H^+ exchanger; pH_i, intracellular pH; EL, extracellular loop; IL, intracellular loop; TM, transmembrane spanning region; ER, endoplasmic reticulum; MTS-2, 1,2-ethanediyl-bis-methanethiosulfonate; MTS-6, 1,6-hexanediyl-bis-methanethiosulfonate; MTS-17, 3,6,9,12,15,-pentaoxaheptadecane-1,17-diyl-bis-methanethiosulfonate; MTSET, 2-(trimethylammonium) ethyl methanethiosulfonate; PMA, phorbol 12-myristate 13-acetate; EIPA, 5-(*N*-ethyl-*N*-isopropyl)amiloride; NHS-LC-biotin, succinimidyl-6-(biotinamide)-hexanoate; $DiOC_6(3)$, 3,3′-dihexyloxacarbocyanine iodide; BCECF-AM, 2′,7′-bis-(2-carboxyethyl)-5(6)-carboxyfluorescein acetoxymethyl ester; HA, hemaglutinin; PCR, polymerase chain reaction; DMEM, Dulbecco's modified Eagle's medium; HEPES, 2-[4-(2-hydroxyethyl)-1-piperazinyl]ethanesulfonic acid; Tris, Tris(hydroxymethyl)aminomethane; EDTA, ethylenediamine-*N*,*N*,*N*′,*N*′-tetraacetic acid; PBS, phosphate-buffered saline; PAGE, polyacrylamide gel electrophoresis; SH, sulfhydryl; LDS, lithium dodecylsulfate; CCD, charge coupled device; aa, amino acid.

10.1021/bi0608616 CCC: $33.50
Published on Web 10/17/2006

subunits may be required for NHE1 function using several kinetic approaches (*12*−*14*). In addition, the sigmoidal cytosolic H^+ dependence has recently been reported to be best explained by an allosteric model involving the cooperative interaction between subunits (*14*).

In this study, we have addressed whether dimerization is responsible for the activity of NHE1. We found that expression of a dominant-negative mutant exchanger greatly inhibited the exchange activity in the neutral pH_i range by inducing an acidic shift of the pH_i dependence. Furthermore, the exchange activity was markedly reduced by intermolecular cross-linking between engineered cysteine residues, suggesting that cross-linking restricts the cooperative movement between NHE1 subunits and thereby inhibits ion transport. The present findings provide a strong piece of evidence that dimerization is required for the physiological function of NHE1.

EXPERIMENTAL PROCEDURES

Antibodies and Other Materials. The polyclonal antibody against human NHE1 has been described previously (*15*). Antibodies against HA (3F10) and c-Myc epitopes were purchased from Roche Diagnostics GmbH (Germany) and Santa Cruz Biotechnology, Inc. (CA), respectively. Cysteine-modifier reagent MTSET and cross-linkers MTS-2, MTS-6, and MTS-17 were purchased from Toronto Research Chemicals, Inc. (Canada). ^{22}NaCl and [^{14}C]-benzoic acid were purchased from Perkin-Elmer Life Science, Inc. (MA). All other chemicals were of the highest purity available.

Cell Culture and Plasmid DNA Transfection. The exchanger-deficient cell line (PS120) (*16*) and corresponding transfectants were maintained in DMEM containing 25 mM $NaHCO_3$ and supplemented with 7.5% (v/v) fetal calf serum, penicillin (50 units/mL), and streptomycin (50 μg/mL). Cells were maintained at 37 °C in the presence of 5% CO_2. All cDNA constructs were transfected into PS120 or CCL39 cells using the calcium phosphate-DNA coprecipitation technique or with Lipofectamine 2000 (Invitrogen Corp., CA), and stable clones for NHE1 and mutant constructs were selected by repetitive H^+-killing selection procedures, as described previously (*17*). In some cases, G418-resistant cell clones were isolated.

Construction of the NHE1 Mutant Plasmid. A plasmid carrying a cDNA encoding human NHE1 and containing unique restriction sites cloned into the mammalian expression vector pECE has been described previously (*17*). A cDNA construct for NHE1 in which all endogenous cysteine residues were replaced by alanine, designated as Cys-less NHE1, has also been described previously (*18*). Construction of plasmids for NHE1 containing point mutations was carried out by a PCR-based strategy using two template plasmids encoding wild-type or Cys-less NHE1, as described previously (*18*). Similarly, plasmids containing nucleotide sequences corresponding to the HA epitope YPYDVPDYAS or the c-Myc epitope EQKLISEEDL were constructed by inserting PCR fragments produced using antisense primers containing either epitope sequence and a stop codon just after the *C*-terminus of NHE1 into the appropriate restriction sites of the plasmid containing NHE1 cDNA. Constructs were confirmed by sequencing plasmids with an ABI-PRISM DNA sequencer model 3100 (Applied Biosystems, CA). In this study, we use the prefix "cl-" for point mutants produced from Cys-less NHE1 as background.

Cross-Linking between Cysteine Residues of NHE1. The cross-linking reaction was performed using PS120 cells stably expressing the NHE1 mutants, essentially as described previously (*11*). Cells expressing each mutant containing a single cysteine residue at an extracellular site of Cys-less NHE1 were grown to confluence, usually on a 12-well plate, and then were washed twice with balanced salt solution (BSS) containing 136 mM NaCl, 4 mM KCl, 1 mM $MgCl_2$, 1.8 mM $CaCl_2$, 5 mM glucose, and 10 mM HEPES at pH 7.4 adjusted with NaOH. Cells were then treated with various thiol-specific cross-linkers, MTS-2, MTS-6, and MTS-17 (usually 0.1−1.0 mM), in the above solution for 15 min at room temperature. The cross-linking reaction was stopped by the addition of 300 μL of 2× LDS sample buffer (Invitrogen) containing 10 mM *N*-ethylmaleimide per well, and then the PAGE mobility of NHE1 variants in the samples was analyzed by immunoblotting.

Immunoprecipitation and Immunoblotting. For co-immunoprecipitation of the Myc-tagged wild-type NHE1 and the HA-tagged E262I mutant, cells coexpressing these proteins were washed with ice-cold PBS and solubilized with lysis buffer (1% Triton X-100, 5 mM EDTA, 1 mM phenylmethylsulfonyl fluoride, and 1 mM benzamidine in PBS) for 20 min on ice. Quantitative analysis revealed that most of NHE1 (88 ± 4%) was recovered in the Triton-soluble fraction. After centrifugation for 5 min at 15,000 rpm, the supernatant (Triton-soluble fraction) was incubated for 2 h at 4 °C with rabbit anti-Myc antibody plus 30 μL of Protein A-Sepharose beads (Amersham Biosciences, Inc., NJ). The beads were washed five times with ice-cold lysis buffer, and proteins were eluted with LDS sample buffer containing 50 mM DTT. After PAGE on 3−8% gradient gels (NuPAGE Gel, Invitrogen), proteins were transferred electrophoretically onto polyvinylidene difluoride membranes and subjected to immunoblotting with anti-HA. Proteins were visualized by enhanced chemiluminescence detection (Amersham).

Immunocytochemistry. Cells were fixed with cold methanol and then blocked with PBS containing 5% BSA fraction IV. Cells were then treated with anti-NHE1 or anti-HA antibody followed by fluorescent staining with a rhodamine-labeled secondary antibody. Fluorescent images were taken using a confocal laser scanning attachment (MRC1024, BioRad) mounted on an upright microscope (BX50WI, Olympus Corp., Japan) equipped with an 60× water immersion objective (LUMPlanFI, Olympus). Both the anti-NHE1 antibody and the secondary antibody were used after absorbing against PS120 cells. All procedures were performed at room temperature.

Surface Labeling. Cells were incubated with 1 mM NHS-LC-Biotin (Pierce Biotechnology, IL) in PBS containing 0.1 mM $CaCl_2$ and 1 mM $MgCl_2$ for 30 min at room temperature and then solubilized with lysis buffer. The lysate was centrifuged to remove the insoluble fraction. The supernatant was incubated with streptavidin-agarose beads (Pierce) for 1 h at 4 °C, and the beads were then washed five times with lysis buffer. The proteins were eluted with 2× LDS sample buffer by heating and then subjected to immunoblot analysis.

Measurement of ^{22}Na Uptake. $^{22}Na^+$ uptake activity was measured by the K^+/nigericin pH_i clamp method (*19*). Briefly, serum-depleted cells in 24-well plates were preincubated

for 30 min at 37 °C in a Na^+-free choline chloride/KCl medium containing 20 mM HEPES/Tris (pH 7.4), 1.2−140 mM KCl, 2 mM $CaCl_2$, 1 mM $MgCl_2$, 5 mM glucose, and 5 μM nigericin (Invitrogen). $^{22}Na^+$ uptake was started by adding the same choline chloride/KCl solution containing $^{22}NaCl$ (37 kBq/mL: final concentration, 1 mM), 1 mM ouabain, and 0.1 mM bumetanide. In some wells, the uptake solution contained 0.1 mM EIPA. One to 5 min later, cells were rapidly washed four times with ice-cold PBS to terminate $^{22}Na^+$ uptake. pH_i was calculated from $[K^+]_i/[K^+]_o = [H^+]_i/[H^+]_o$ by assuming an intracellular $[K^+]$ of 120 mM. In some experiments, cells were treated with MTS cross-linkers for 15 min at room temperature prior to incubation with pH_i-clamp buffer. The data were normalized on the basis of protein concentration, which was measured using a bicinchoninic assay system (Pierce), using bovine serum albumin as a standard.

Intracellular pH Measurement. Cells were seeded onto 22-mm glass coverslips coated with collagen Type-I (BD Biosciences, NJ). Two days after plating, cells were loaded with 1 μM BCECF/AM (Invitrogen) in a "Na^+ solution" containing 10 mM HEPES/Tris (pH 7.4), 136 mM NaCl, 4 mM KCl, 1.8 mM $CaCl_2$, 1 mM $MgCl_2$, and 5 mM glucose for 10 min at room temperature. The coverslip was mounted on a flow chamber and continuously perfused with solution at 0.6 mL/min by means of a Perista pump (ATTO Corp., Japan). Changes in pH_i were estimated by ratiometric imaging of changes in BCECF fluorescence. Fluorescence was monitored at 510−530 nm by alternatively exciting at 440 and 490 nm through a 505-nm dichroic reflector. Fluorescence images were collected every 5 or 10 s using a cooled CCD camera (ORCA-ER, Hamamatsu photonics K.K., Japan) mounted on an inverted microscope (IX 71, Olympus) with an 20× objective (UApo/340, Olympus) and then were processed with AQUACOSMOS software (Hamamatsu photonics). For NH_4 prepulse, cells were perfused for 5 min with the above Na^+ solution containing 30 mM NH_4Cl, followed by perfusion with a Na^+-free solution (NaCl was replaced by choline Cl). The NHE1-dependent pH_i recovery was induced by reperfusion with the Na^+ solution. The pH_i value was calibrated using a "high K^+ solution" containing 5 μM nigericin adjusted to various pH values. The change in pH_i was also measured by the [^{14}C]benzoic acid-equilibration method (*17*). In this experiment, serum-depleted cells were preincubated for 30 min in bicarbonate-free HEPES-buffered DMEM (pH 7.0) and then incubated in the same medium containing [^{14}C]benzoic acid (1 μCi/mL) for 10 min at 37 °C. After washing four times with ice-cold PBS, the cellular uptake of ^{14}C-radioactivity was measured. The change in pH_i was calculated as described previously (*17*).

RESULTS

Heterodimer Formation between the Wild-Type and Inactive Mutant Exchangers. In this study, we constructed two NHE1 mutants, G309V and E262I (see Figure 1A for their positions in the secondary structure of NHE1). These mutant exchangers showed no EIPA-sensitive $^{22}Na^+$ uptake activity when they were expressed in exchanger-deficient PS120 cells (Figure 1B). Although the fully glycosylated mature form of the wild-type and E262I exchangers were recognized in the immunoblot with anti-NHE1 antibody (Figure 1C), only the immature form of G309V was observed in the immunoblot, suggesting that G309V may be retained in the intracellular membranes. In order to check the surface expression of these mutant exchangers, we carried out the immunofluorescence analysis with anti-NHE1 antibody. Similar to the wild-type NHE1, E262I tagged with HA were expressed at least partly in the plasma membrane, as shown by immunofluorescence observation with anti-HA antibody (Figure 2A; see inset for the fluorescence intensity profile analysis). In contrast, most of G309V proteins were retained in the intracellular membranes (Figure 2A and B for summarized data). Furthermore, G309V proteins were mostly co-stained with the ER marker $DiOC_6(3)$, whereas neither the wild-type nor the E262I exchangers were co-stained (Figure 2C). Thus, the lack of exchange activity of G309V could result from no surface expression of this mutant.

In order to examine whether the G309V mutant interacts with the wild-type NHE1 and thus inhibit its plasma membrane trafficking, we isolated a stable cell line expressing

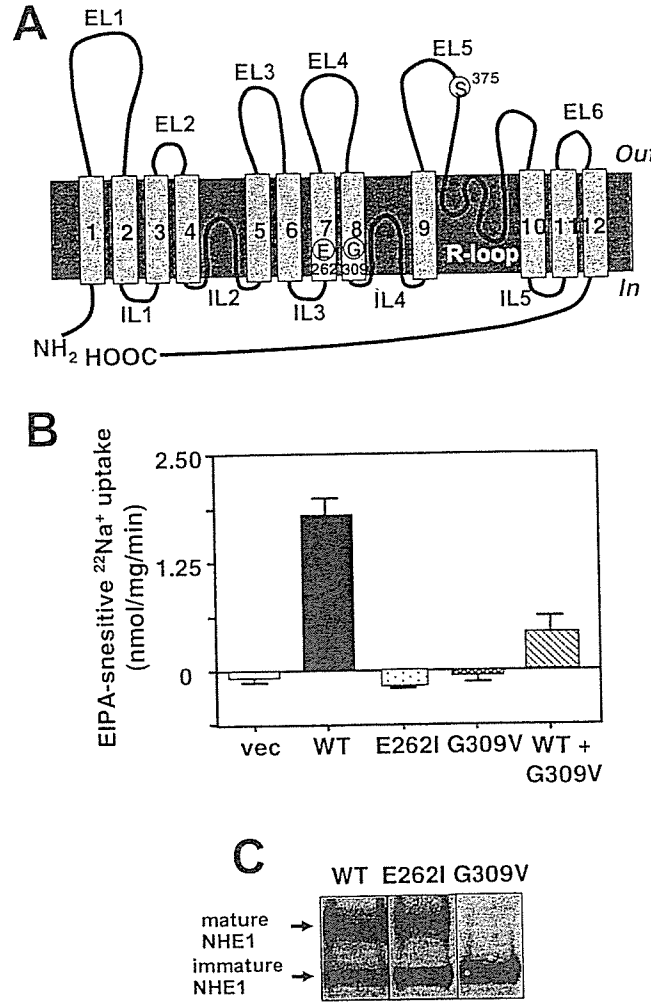

FIGURE 1: Characterization of two inactive mutant exchangers. (A) Secondary structure model of NHE1. The membrane topology has previously been determined by cysteine-accessibility analysis (*18*). Relative positions of mutated residues (Glu^{262}, Gly^{309}, and Ser^{375}) are indicated in the Figure. R-loop, reentrant loop. (B) EIPA-sensitive $^{22}Na^+$-uptake activity in PS120 cells transiently transfected with an empty pECE vector (vec), wild-type NHE1 (WT), E262I, G309V, or wild-type NHE1 plus G309V (0.3 μg for each). Values are the means ± S.D. of triplicate determinations. (C) Immunoblots of proteins obtained from cells stably expressing the wild-type, E262I, or G309V. Cell lysate proteins (50 μg/lane) were applied to 3−8% SDS-PAGE and visualized with anti-NHE1 antibody.